Discrete Ordinate Theory of Radiative Transfer

I. Rayleigh Scattering

By Gilbert N. Plass, George W. Kattawar, and Frances E. Catchings

The research described in this report was

funded by the

National Aeronautics and Space Administration

Contract No. NGR 44-001-117

Department of Physics
Texas A&M University
College Station, Texas 77843

October 15, 1971

A paper based on the material in this report has been submitted to the Journal of Atmospheric Sciences.

Discrete Ordinate Theory of Radiative Transfer
I. Rayleigh Scattering

Gilbert N. Plass, George W. Kattawar, and Frances E. Catchings

Department of Physics, Texas A&M University, College Station, Texas 77840

ABSTRACT

An entirely rigorous method for the solution of the equations for radiative transfer is presented based on the discrete ordinate theory. The advantages of the present method are: 1. all orders of multiple scattering are calculated at once; 2. layers of any thickness may be combined, so that a realistic model of the atmosphere can be developed from any arbitrary number of layers, each with different properties and thicknesses; 3. calculations can readily be made for large optical depths and with highly anisotropic phase functions; 4. results are obtained for any desired value of the surface albedo including the value unity and for a large number of polar and azimuthal angles including the polar angle $\theta = 0^{\circ}$; 5. all fundamental equations can be interpreted immediately in terms of the physical interactions appropriate to the problem. Both the general theory and the method of calculation are discussed. As a first example of the method numerous curves are given for both the reflected and transmitted radiance for Rayleigh scattering from a homogeneous layer for a range of optical thicknesses from 0.0019 to 4096, surface albedo A = 0, 0.2, and 1, and cosine of solar zenith angle $\mu = 1$, 0.5379, and 0.1882.

1. Introduction

The radiation field arising from multiple scattered photons in a planetary atmosphere is of great practical interest. Elegant and elaborate mathematical solutions have been developed for isotropic and Rayleigh scattering by Chandrasekhar (1960), Sekera (1956, 1957), Kourganoff (1952), and others. Numerical values for the various parameters of the diffuse radiation from a planetary atmosphere with Rayleigh scattering have been given in a set of tables published by Coulson, Dave, and Sekera (1960). These tables are limited to optical thicknesses of unity or less. Numerical results for Rayleigh scattering have also been presented by Herman and Browning (1965), Dave and Furukawa (1966), Kahle (1968a, b), Howell and Jacobowitz (1970), and Fymat and Abhyankar (1971), among others. Among these authors only Dave and Furukawa (1966) and Kahle (1968b) give radiance values for an optical thickness as large as 10. Most of the published results are for a surface albedo of zero.

More realistic problems for planetary atmospheres which take account of the highly anisotropic scattering from aerosols as well as the variations in the atmospheric parameters with height have not been successfully solved in terms of standard mathematical functions. Various numerical techniques have also been proposed to calculate the radiance for anisotropic scattering. Some of these methods such as that of Herman et al (1971) appear to be applicable only for small optical thicknesses. Important results using matrix or doubling methods have been given by Twomey et al (1967), Dave and Gazdag (1970), Dave (1970), Hansen (1969a, b, 1971a, b), and Hansen and Pollack (1970). As interesting as they are, these results are limited by various factors. Those of Twomey et al (1967) use a phase function that is averaged over a range of angles. Most of these authors use a doubling method which is applicable to homogenous layers, but has not been applied as yet to the real atmosphere where various parameters vary with height. Furthermore in most of these methods, each order of multiple scattering must be calculated separately and finally added together.

The discrete ordinate theory has several important advantages over these other methods. The general theory of discrete spaces has been presented by Preisendorfer (1965). Important contributions to the theory have been made by Twomey et al (1966) and more recently by Grant and Hunt (1969). Our method is closely related to that of Grant and Hunt, but incorporates various improvements and develops a very much simpler expression for the radiance within a layer.

A particularly simple form of the discrete ordinate theory is presented here that is especially designed for application to physical problems of radiative transfer. This is an entirely rigorous method for the solution of the equations for radiative transfer. The theory given here has the following important advantages: 1. all orders of multiple scattering are calculated at once with a corresponding reduction in computer time over methods involving iterations; 2. layers of any thickness may be combined, so that a realistic model of the atmosphere may be developed from any arbitrary number of layers of any predetermined thicknesses, each with different properties; 3. calculations can readily be made for large optical depths and with highly anisotropic phase functions; 4. results are obtained for any desired value of the surface albedo including the value unity as well as for any polar angle which corresponds to one of the set given by the Lobatto integration scheme for the number of integration points chosen (the polar angle

$\theta = 0^{\circ}$ is always included in the set); 5. all fundamental equations can be interpreted immediately in terms of the physical interactions appropriate to the problem.

After presentation of the general theory and the method of numerical calculation, results are given for Rayleigh scattering from a homogeneous layer. Further papers in this series will present results for other cases, including more anisotropic phase functions and inhomogeneous atmospheres.

1. Discrete Ordinate Theory

In a plane parallel medium all properties depend on a single spatial coordinate x. For convenience the position within the medium is denoted by the optical depth τ, defined as the distance x within the medium divided by the attenuation length. Divide the medium into any desired number of layers; the boundaries between layers are indicated in order from the top of the medium by the value of the optical depth at the boundary τ_0, τ_1, τ_2. The medium may be inhomogeneous within any layer (see Fig. 1).

Let $I^+(\tau)$ be the specific intensity at the optical depth τ for the radiation in the downward direction according to the usual definition. In discrete ordinate theory $I^+(\tau)$ is a column matrix

$$I^+(\tau) = \begin{bmatrix} I^+(\tau,\mu_1) \\ I^+(\tau,\mu_2) \\ \cdot \\ \cdot \\ \cdot \\ I^+(\tau,\mu_m) \end{bmatrix} , \tag{1}$$

where $I^+(\tau,\mu_i)$ is the downward intensity at the angle $\theta_i = \cos^{-1}\mu_i$ $(0<\mu_i\leq 1)$. The azimuthal or ϕ dependence can be separated out of the equation as is shown in Section 2 and its inclusion here is unnecessary. Similarly let $I^-(\tau)$ be a column matrix that represents the upward intensity.

Consider the intensities of the radiation emerging from a layer whose boundaries are at τ_0 and τ_1. These intensities, $I^+(\tau_1)$ and $I^-(\tau_0)$, depend linearly on the incident intensities, $I^+(\tau_0)$ and $I^-(\tau_1)$, and the contribution from the sources within the layer, $J^+(\tau_0,\tau_1)$ and $J^-(\tau_1,\tau_0)$ (the downward intensity at τ_1 and the upward intensity at τ_0 due to sources within the layer). Except when it is necessary to emphasize the dependence on τ, we use the following concise notation: $I^-_0 = I^-(\tau_0)$, $I^+_0 = I^+(\tau_0)$, $I^-_1 = I^-(\tau_1)$, $I^+_1 = I^+(\tau_1)$, $J^+_{01} = J^+(\tau_0,\tau_1)$, and $J^-_{10} = J^-(\tau_1,\tau_0)$.

Thus

$$I^+_1 = t_{01}I^+_0 + r_{10}I^-_1 + J^+_{01}, \tag{2a}$$

$$I^-_0 = r_{01}I^+_0 + t_{10}I^-_1 + J^-_{10}, \tag{2b}$$

where $t_{01} = t(\tau_0,\tau_1)$ is a diffuse transmission operator and $r_{01} = r(\tau_0,\tau_1)$ is a diffuse reflection operator. For homogeneous layers $r_{01} = r_{10}$ and $\tau_{01} = \tau_{10}$, but these relations no longer hold in general for inhomogeneous layers. The operators r and t are $\ell \times \ell$ matrices which multiply the column vectors I.

The problem treated in this section is the derivation of the expression for the diffuse reflection and transmission operators for a combined layer (from τ_0 to τ_2) from the known operators for two separate layers (from τ_0 to τ_1 and from τ_1 to τ_2). The resulting expression is valid for the combination of any two layers of finite size and different properties. In the next section the relation between these operators and the local physical properties (single scattering function and single scattering albedo) are derived.

Equations similar to Eq. (2) are valid for the emerging flux of the layer from τ_1 to τ_2

$$I^+_2 = t_{12}I^+_1 + r_{21}I^-_2 + J^+_{12}, \tag{3a}$$

$$I^-_1 = r_{12}I^+_1 + t_{21}I^-_2 + J^-_{21} \tag{3b}$$

and also for the combined layer from τ_0 to τ_2

$$I^+_2 = t_{02}I^+_0 + r_{20}I^-_2 + J^+_{02}, \tag{4a}$$

$$I^-_0 = r_{02}I^+_0 + t_{20}I^-_2 + J^-_{20}. \tag{4b}$$

Multiply Eq. (2a) by r_{12} from the left, add this equation to Eq. (3b), and multiply the resulting equation from the left by $(E - r_{12}r_{10})^{-1}$, where E is the identity matrix, to obtain

$$I^-_1 = (E - r_{12}r_{10})^{-1} [t_{21}I^-_2 + r_{12}t_{01}I^+_0 + J^-_{21} + r_{12}J^+_{01}] \tag{5}$$

This equation relates the upward flux at any interior point τ_1 in the layer from τ_0 to τ_2 with the incident upward and downward flux, I^-_2 and I^+_0 respectively, at the boundaries and the source functions for the layers. The physical interpretation of this type of equation is discussed later.

Multiply Eq. (3b) by r_{10} from the left, add this equation to Eq. (2a), and multiply the resulting equation from the left by $(E - r_{10}r_{12})^{-1}$ to obtain

$$I^+_1 = (E - r_{12}r_{10})^{-1} [t_{01}I^+_0 + r_{10}t_{21}I^-_2 + J^+_{01} + r_{10}J^-_{21}]. \tag{6}$$

This expression gives the downward flux at any interior point τ, in the layer from τ_0 to τ_2.

Substitute the expression for I^+_1 from Eq. (6) into Eq. (3a). The resulting equation expresses I^+_2 in terms of I^+_0, I^-_2, and J^+_{02}. A comparison of the coefficients of these quantities with Eq. (4a) yields the following expressions

$$t_{02} = t_{12}(E - r_{10}r_{12})^{-1} t_{01}, \tag{7a}$$

$$r_{20} = r_{21} + t_{12}(E - r_{10}r_{12})^{-1}\, r_{10}r_{21}, \tag{8a}$$

$$J^{+}_{02} = J^{+}_{12} + t_{12}(E - r_{10}r_{12})^{-1}\, (J^{+}_{01} + r_{10}J^{-}_{21}). \tag{9a}$$

Similarly the substitution of the expression for I^{-}_{1} from Eq. (5) into Eq. (2b) and comparison of this result with Eq. (4b) yields:

$$t_{20} = t_{10}(E - r_{12}r_{10})^{-1}\, t_{21}, \tag{7b}$$

$$r_{02} = r_{01} + t_{10}(E - r_{12}r_{10})^{-1}\, r_{12}t_{01}, \tag{8b}$$

$$J^{-}_{20} = J^{-}_{10} + t_{10}(E - r_{12}r_{10})^{-1}\, (J^{-}_{21} + r_{12}J^{+}_{01}). \tag{9b}$$

The physical meaning of these equations is found if a formal expansion of the quantity $(E - r_{10}r_{12})^{-1}$ is made

$$(E - r_{10}r_{12})^{-1} = \sum_{k=0}^{\infty} (r_{10}r_{12})^{k}. \tag{10}$$

Substitution of this expression in Eq. (8a), for example, yields

$$r_{20} = r_{21} + t_{12} \sum_{k=0}^{\infty} (r_{10}r_{12})^{k}\, r_{10}t_{21}. \tag{11}$$

According to Eq. (4a), r_{20} gives the contribution to the downward flux at the lower boundary, I^{+}_{2}, from an incident upward flux I^{-}_{2}. The contribution from the term $k = j$ in Eq. (11) corresponds to radiation that has been diffusely reflected from the layer (τ_0,τ_1) j times. Equation (11) states that the radiation reflected from the layer (τ_0,τ_2) is equal to the radiation reflected directly from the layer (τ_1,τ_2), r_{21}, to which is added the radiation which undergoes diffuse transmission through the lower layer, t_{21}, times the diffuse reflection from the upper layer, r_{10}, times j diffuse reflections from the lower and then the upper layer, $(r_{10}r_{12})^{j}$, times the diffuse transmission through the lower layer, t_{12}.

The physical meaning of each of the other expressions for the diffuse transmittance, reflectance, and emittance is obtained in the same manner. One advantage of the discrete ordinate method is that each quantity in the final equations has a direct physical meaning. The key results are given by Eqs. (7-9), which give expressions for the diffuse transmittance, reflectance, and emittance for the combination of any two atmospheric layers of arbitrary thickness. The upward and downward diffuse intensity at the boundary of the combined layer is obtained from Eq. (4). The diffuse intensity at any point within a layer is given by Eqs. (5) and (6), an expression appreciably simpler than those previously given in the literature (Grant and Hunt, 1969). The physical meaning of each term in these equations is obtained by the same method as discussed in connection with Eq. (8a). For example, the upward diffuse flux at the interior point τ, is given by Eq. (5) as (1) the reflection to every order between the layers of contributions from the upward diffuse intensity at the lower boundary τ_2 transmitted through the lower layer (1,2), (2) the downward diffuse intensity at the upper boundary τ_0 transmitted through the upper layer (0,1) and reflected from the lower layer (1,2), (3) the upward diffuse emission of the layer (1,2), and (4) the downward diffuse emission from the upper layer (0,1) reflected from the lower layer (1,2) as represented by the first, second, third, and fourth terms of the right hand bracket in Eq. (5) respectively.

Any reflecting properties of a lower boundary surface can easily be included in the formalism. A layer extending from τ_0 to τ_1 can be combined with a lower boundary surface if the diffuse transmission and reflection operator can be defined. Consider the lower surface as extending from τ_1 to τ_2.

The boundary condition is that $I^+_2 = I^-_2 = 0$, i.e. no radiation either leaves or is incident on the τ_2 boundary of the ground. The appropriate transmission and reflection operators are $t_{12} = t_{21} = 0$ and $r_{12} = r_{21} = r_G$. Thus, it follows from Eq. (2) that

$$I^-_1 = r_G I^+_1. \tag{12}$$

The matrix r_G is determined for any surface by calculation of the diffuse intensity reflected at every angle from a given downward intensity at a particular angle of incidence. The angle of incidence is then varied through all values considered in the problem. The albedo of the surface is obtained from the ratio of the upward flux to the downward flux at the surface. The elements of r_G in a given column are all equal for a Lambert surface.

2. Numerical Techniques

The theory is extended in this section to include the case where the radiance depends on both μ and ϕ. Fourier analysis is used to decouple the azimuth dependence in the equations. Consider the equation of transfer for the diffuse radiance $I(\tau;\mu,\phi)$ i.e.,

$$(\mu \frac{d}{d\tau} + 1)I(\tau;\mu,\phi) = F \exp(-\tau/\mu_0)\omega(\tau)p(\tau;\mu,\phi;\mu_0,\phi_0) + \int_{-1}^{1}\int_{0}^{2\pi} p(\tau;\mu,\phi;\mu',\phi')I(\tau;\mu',\phi')d\mu'd\phi' \tag{13}$$

where F is the incident solar flux, ω is the single scattering albedo, and $-1 \leq \mu \leq 1$ and $0 \leq \omega(\tau) \leq 1$. The phase function $p(\tau;\mu,\phi;\mu_0,\phi_0)$ is subject to the following normalization condition

$$\int_{-1}^{1}\int_{0}^{2\pi} p(\tau;\mu,\phi;\mu',\phi')d\mu'd\phi' = 1. \tag{14}$$

Since the phase function depends only on the cosine of the angle between the directions (μ,ϕ) and (μ',ϕ'), then

$$\begin{aligned} p(\mu,\phi;\mu',\phi') &= p(\mu,\phi';\mu',\phi), \\ p(-\mu,\phi;-\mu',\phi') &= p(\mu,\phi;\mu',\phi'), \\ p(\mu,\phi;-\mu',\phi') &= p(-\mu,\phi;\mu',\phi') = p(\mu',\phi',-\mu,\phi). \end{aligned} \tag{15}$$

The standard Legendre polynomial expansion technique (Chandrasekhar, 1960) is used to decouple the ϕ dependence. Assume that the phase function consists of only a finite number of terms N, so that

$$p(\cos \Theta) = \sum_{\ell=0}^{N} p_\ell(\mu,\mu') \cos \ell (\phi-\phi'). \tag{16}$$

This equation together with Eq. (14) yields

$$\int_{-1}^{1} p_0(\mu,\mu')d\mu' = (2\pi)^{-1} \tag{17}$$

for all $0 < \mu \leq 1$. Assume that the radiance I has a similar expansion, namely

$$I(\tau,\mu,\phi) = \sum_{\ell=0}^{N} I_\ell(\tau,\mu) \cos \ell\, (\phi-\phi_0). \tag{18}$$

This expansion together with Eqs. (16) and (13) yields

$$\begin{aligned}(\mu\frac{d}{d\tau} + 1)I_\ell(\tau,\mu) &= \omega(\tau)\ F \exp\ (-\tau/\mu_0)p_\ell(\mu,\mu_0)\\ &+ \pi(1 + \delta_{0\ell}) \int_{-1}^{1} p_\ell(\mu,\mu')I_\ell(\tau,\mu')d\mu'\end{aligned} \tag{19}$$

for $\ell = 0, 1, 2, \ldots, N$. We have thus reduced Eq. (13) to a system of $N + 1$ independent equations. Rewriting Eq. (19) in terms of the upward (I^-) and downward (I^+) radiance we have

$$\begin{aligned}(\mu\frac{d}{d\tau} + 1)I_\ell^+(\tau,\mu) &= \omega(\tau)\ F \exp\ (-\tau/\mu_0)p_\ell(\mu,\mu_0)\\ &+ \omega(\tau)\pi(1 + \delta_{0\ell})\ \{\int_0^1 p_\ell(\mu,\mu')I_\ell^+(\tau,\mu')d\mu'\\ &+ \int_0^1 p_\ell(\mu,-\mu')I_\ell^-(\tau,\mu')d\mu'\},\end{aligned} \tag{20}$$

$$\begin{aligned}(-\mu\frac{d}{d\tau} + 1)I_\ell^-(\tau,\mu) &= \omega(\tau)\ F \exp\ (-\tau/\mu_0)p_\ell(-\mu,\mu_0)\\ &+ \omega(\tau)\pi(1 + \delta_{0\ell})\ \{\int_0^1 p_\ell(-\mu,\mu')I_\ell^+(\tau,\mu')d\mu'\\ &+ \int_0^1 p_\ell(-\mu,-\mu')I_\ell^-(\tau,\mu')d\mu'\}.\end{aligned}$$

In discrete ordinate theory the integrals are discretized by some appropriate quadrature formula. In all the calculations reported in this article Lobatto integration is used since it allows computations of the radiance at $\mu = \pm 1$. The quadrature is performed as follows:

$$\int_{-1}^{1} g(\mu)d\mu = \sum_{j=1}^{n} g(\mu_j)c_j + R_n, \tag{21}$$

where the error term R_n vanishes for a polynomial of degree $\leq 2n - 3$.

The abscissas μ_j and weights c_j were taken from Stroud and Secrest (1966). Let us adopt the following matrix notation for the discrete ordinate case

$$\underset{\sim}{I}_\ell^{+}(\tau,\mu_i,\mu_j) = \begin{bmatrix} I_{11}^{+\ell} & I_{12}^{+\ell} & \cdots & I_{1m}^{+\ell} \\ \vdots & \vdots & & \vdots \\ I_{m1}^{+\ell} & I_{m2}^{+\ell} & \cdots & I_{mm}^{+\ell} \end{bmatrix},$$

$$\underset{\sim}{P}_\ell^{++}(\tau,\mu_i,\mu_j) = \begin{bmatrix} P_{\ell 11}^{++} & P_{\ell 12}^{++} & \cdots & P_{\ell 1m}^{++} \\ \vdots & \vdots & & \vdots \\ P_{\ell m1}^{++} & P_{\ell m2}^{++} & \cdots & P_{\ell mm}^{++} \end{bmatrix},$$

$$\underset{\sim}{P}_\ell^{+-}(\tau,\mu_i,-\mu_j) = \begin{bmatrix} P_{\ell 11}^{+-} & P_{\ell 12}^{+-} & \cdots & P_{\ell 1m}^{+-} \\ \vdots & \vdots & & \vdots \\ P_{\ell m1}^{+-} & P_{\ell m2}^{+-} & \cdots & P_{\ell mm}^{+-} \end{bmatrix}, \qquad (22)$$

$$\underset{\sim}{J}_\ell^{+}(\tau,\mu_i,\mu_j) = F\omega(\tau) \begin{bmatrix} P_{\ell 11}^{++}\exp(-\tau/\mu_1) & \cdots & P_{\ell 1m}^{++}\exp(-\tau/\mu_m) \\ \vdots & & \vdots \\ P_{\ell m1}^{++}\exp(-\tau/\mu_1) & \cdots & P_{\ell 1m}^{++}\exp(-\tau/\mu_m) \end{bmatrix},$$

$$\underset{\sim}{J}_\ell^{-}(\tau,\mu_i,-\mu_j) = F\omega(\tau) \begin{bmatrix} P_{\ell 11}^{+-}\exp(-\tau/\mu_1) & \cdots & P_{\ell 1m}^{+-}\exp(-\tau/\mu_m) \\ \vdots & & \vdots \\ P_{\ell m1}^{+-}\exp(-\tau/\mu_1) & \cdots & P_{\ell mm}^{+-}\exp(-\tau/\mu_m) \end{bmatrix},$$

$$\underset{\sim}{c} = \left[c_j\delta_{jk}\right],$$

$$\underset{\sim}{M} = \left[\mu_j\delta_{jk}\right],$$

where $\mu_i > 0$, $m = n/2$ (n is the order of the quadrature in Eq. (21)) and each column in the radiance matrix corresponds to a different angle of incidence for the source.

Equation (20) in this representation becomes

$$\underset{\sim}{M}\,\frac{d\underset{\sim}{I}_\ell^{+}(\tau)}{d\tau} + \underset{\sim}{I}_\ell^{+}(\tau) = \underset{\sim}{J}_\ell^{+}(\tau) + \omega(\tau)\pi(1 + \delta_{0\ell})x$$

$$\{\underset{\sim}{p}_\ell^{++}(\tau)\underset{\sim}{c}\underset{\sim}{I}_\ell^{+}(\tau) + \underset{\sim}{p}_\ell^{+-}(\tau)\underset{\sim}{c}\underset{\sim}{I}_\ell^{-}(\tau)\}, \tag{23}$$

$$-\underset{\sim}{M}\,\frac{d\underset{\sim}{I}_\ell^{-}(\tau)}{d\tau} + \underset{\sim}{I}_\ell^{-}(\tau) = \underset{\sim}{J}_\ell^{-}(\tau) + \omega(\tau)\pi(1 + \delta_{0\ell})\{\underset{\sim}{p}_\ell^{-+}(\tau)\underset{\sim}{c}\underset{\sim}{I}_\ell^{+}(\tau) + \underset{\sim}{p}_\ell^{--}(\tau)\underset{\sim}{c}\underset{\sim}{I}_\ell^{-}(\tau)\}.$$

With the equation of transfer expressed in this form, the infinitesimal generators of the star semigroup are as follows (see Grant and Hunt, 1969).

$$\begin{aligned}
\underset{\sim}{\Gamma}_\ell^{++}(\tau) &= \underset{\sim}{M}^{-1}[\underset{\sim}{E} - \omega(\tau)\pi(1 + \delta_{0\ell})\underset{\sim}{p}_\ell^{++}(\tau)\underset{\sim}{c}],\\
\underset{\sim}{\Gamma}_\ell^{+-}(\tau) &= \underset{\sim}{M}^{-1}\omega(\tau)\pi(1 + \delta_{0\ell})\underset{\sim}{p}_\ell^{+-}(\tau)\underset{\sim}{c},\\
\underset{\sim}{\Gamma}_\ell^{-+}(\tau) &= \underset{\sim}{M}^{-1}\omega(\tau)\pi(1 + \delta_{0\ell})\underset{\sim}{p}_\ell^{-+}(\tau)\underset{\sim}{c},\\
\underset{\sim}{\Gamma}_\ell^{--}(\tau) &= \underset{\sim}{M}^{-1}[\underset{\sim}{E} - \omega(\tau)\pi(1 + \delta_{0\ell})\underset{\sim}{p}_\ell^{--}(\tau)\underset{\sim}{c}],\\
\underset{\sim}{\Sigma}_\ell^{+}(\tau) &= \underset{\sim}{M}^{-1}\underset{\sim}{J}_\ell^{+}(\tau),\\
\underset{\sim}{\Sigma}_\ell^{-}(\tau) &= \underset{\sim}{M}^{-1}\underset{\sim}{J}_\ell^{-}(\tau),
\end{aligned} \tag{24}$$

where $\underset{\sim}{E}$ denotes the identity matrix.

It should be noted that due to the symmetry conditions of the phase function (see Eq. (15)) that $\underset{\sim}{\Gamma}_\ell^{++} = \underset{\sim}{\Gamma}_\ell^{--}$ and $\underset{\sim}{\Gamma}_\ell^{+-} = \underset{\sim}{\Gamma}_\ell^{-+}$. This symmetry leads to reciprocity in the equation of transfer. The operators $\underset{\sim}{r}$ and $\underset{\sim}{t}$ for an infinitesimal layer can now be expressed as follows:

$$
\begin{aligned}
\underset{\sim}{t}_{10} &= \underset{\sim}{E} - \underset{\sim}{\Gamma}_{\ell}^{++}(\xi)\Delta_{10} + 0(\Delta_{10}), \\
\underset{\sim}{t}_{01} &= \underset{\sim}{E} - \underset{\sim}{\Gamma}_{\ell}^{--}(\xi)\Delta_{10} + 0(\Delta_{10}), \\
\underset{\sim}{r}_{01} &= \underset{\sim}{\Gamma}_{\ell}^{+-}(\xi)\Delta_{10} + 0(\Delta_{10}), \\
\underset{\sim}{r}_{10} &= \underset{\sim}{\Gamma}_{\ell}^{-+}(\xi)\Delta_{10} + 0(\Delta_{10}),
\end{aligned}
\tag{25}
$$

where $\tau_0 \le \xi \le \tau_1$ and $\Delta_{10} = \tau_1 - \tau_0$. We also have the relations

$$
\begin{aligned}
\Sigma_{01}^{+} &= \Sigma_{\ell}^{+}(\xi)\Delta_{10} + 0(\Delta_{10}), \\
\Sigma_{01}^{-} &= \Sigma_{\ell}^{-}(\xi)\Delta_{10} + 0(\Delta_{10}).
\end{aligned}
\tag{26}
$$

Since the operators for an infinitesimal layer have been defined, the star product algorithm (see Eqs. (7a) - (9b)) can be used to build up a layer of any desired thickness.

In order to insure that the matrices in Eq. (25) are non-negative, the following condition must be satisfied (see Grant and Hunt, 1969).

$$0 \le (\tau_1 - \tau_0) > \min_{\mu_i} \{\mu_i/[1 - \tfrac{1}{2}\omega(\tau)]\}. \tag{27}$$

A value of 2^{-15} for Δ_{10} is chosen in order to insure that the truncation error is small enough for the single scattering approximation to hold. Thus when the thickness of the layer is doubled each time, a value of $\tau = 1$ is reached in fifteen steps.

a. Computational Aspects

The stability of the discrete ordinate algorithm for large optical depths depends on careful attention to several points. The first of these involves the normalization of the phase function (see Eq. (17)). A tabular phase function is used to compute the coefficient $p_\ell(\mu_i,\mu_j)$ in Eq. (16) in the following way:

$$p_0(\mu_i,\mu_j) = \frac{1}{N}\sum_{k=0}^{N-1} p(\mu_i,\mu_j,k\phi),$$

$$p_\ell(\mu_i,\mu_j) = \frac{2}{N}\sum_{k=0}^{N-1} p(\mu_i,\mu_j,k\phi)\ \cos\ (\ell k\phi),\ \ell \neq 0, \tag{28}$$

where $\phi = 2\pi/N$; linear interpolation is used to evaluate the phase function at intermediate points. For each μ_i and μ_j the number of ℓ terms needed is found by successively adding terms in the series expansion until the original phase function has been approximated to the desired accuracy. If $p_0(\mu_i,\mu_j)$ computed in this manner is substituted into Eq. (17), a small error in the normalization is found in general. Furthermore the normalization constant is a function of μ, i.e.,

$$\varepsilon_j = \sum_{i=1}^{n} p_0(\mu_i,\mu_j)c_i - (2\pi)^{-1},\ j = 1,\ 2,\ \ldots,\ m \tag{29}$$

for $0 < \mu_j \leq 1$. A correction matrix is computed from the errors ε_j. This matrix is made symmetric to preserve reciprocity. To insure that this correction matrix is small a large number of quadrature points must be used in the case of a highly anisotropic scattering function.

b. Lambert Surface

By definition a Lambert surface of albedo A converts any radiance distribution impinging upon it into a uniform distribution; if F^+ is the downward flux, then AF^+ is the upward flux. The matrix representation of r_G from Eq. (12) in discrete ordinate theory is

$$r_G = \frac{A}{\sum_{i=1}^{m} c_i\mu_i} \begin{bmatrix} \mu_1 c_1 & \cdots & \mu_m c_m \\ \vdots & & \vdots \\ \mu_1 c_1 & \cdots & \mu_m c_m \end{bmatrix} \tag{30}$$

The only remaining operator to be defined is Σ_G^- which is the source term for the Lambert surface due to the unscattered incident flux. The matrix representation of this operator is given by

$$\Sigma_G^- = \frac{A}{2\pi \sum_{i=1}^{m} c_i\mu_i} \begin{bmatrix} \mu_1 \exp(-\tau/\mu_1) & \cdots & \mu_m \exp(-\tau/\mu_m) \\ \vdots & & \vdots \\ \mu_1 \exp(-\tau/\mu_1) & \cdots & \mu_m \exp(-\tau/\mu_m) \end{bmatrix} . \tag{31}$$

The star product algorithm (Eqs. (7a) - (9b)) can now be used directly by treating the surface extending from τ_1 to τ_2 as a degenerate slab, i.e. $r_{12} = r_{21} = r_G$ and $t_{12} = t_{21} = 0$.

3. Radiance for Rayleigh Scattering

The discrete ordinate method described here has been used to calculate the radiance for Rayleigh scattering. A 42 term Lobatto integration was used which is equivalent to fitting the function with a 81st degree polynomial. The results were printed for each combination of the 21 values of μ and μ_0 as well as for seven ϕ values and 3 different values of the surface albedo A. These values have been checked against all published values of the radiance. In most cases only an approximate check can be made since the values of μ are different for the two calculations; however, in all cases the results agree to within the available accuracy. A different check was made by repeating our calculation with only a 14 term Lobatto integration. These results agree at all optical thicknesses to within 0.2%. The stability of the method was established by noting that for the conservative case flux was conserved to 1 part in 10^6 for optical depths greater than 4000. The incoming solar flux is normalized to unity in our calculations.

The upward radiance when the cosine of the solar zenith angle $\mu_0 = 1$ is shown in Fig. 2a for a surface albedo $A = 0$. There is limb brightening for small values of the optical depth τ; however, when τ is greater than a value near unity, limb darkening occurs. In all of the figures given here for the upward radiance, the curve for the largest τ value in each case is a limiting curve which does not change further by more than the width of the symbol as τ increases further.

The upward radiance when $\mu_0 = 1$ and $A = 0.2$ is given in Fig. 2b. When τ is very small, the upward radiance is essentially constant, since the observed radiation consists almost entirely of photons which have been reflected uniformly in all directions by the Lambert surface and very few which have been scattered in the atmosphere. As τ increases from a small value limb brightening changes to limb darkening when $\tau \sim 1$.

The upward radiance when $\mu_0 = 1$ and $A = 1$ is shown in Fig. 3a. There is relatively little variation with τ; the curve changes from nearly a constant to one with limb darkening as τ increases. For large τ values the ratio of the upward radiance at the zenith to that near the horizon (last computed point $\mu = 0.03785$ or $\theta = 87.83^{\circ}$) is 1.576.

The upward radiance when $\mu_0 = 0.5379$ and $A = 0$ is shown in Fig. 4 for $\phi = 0^{\circ}$ (left hand side) and $\phi = 180^{\circ}$ (right hand side). One particular curve represents the radiance that would be observed in the principal plane from the horizon through the anti-solar point to the zenith and back down to the opposite horizon. One of the most interesting features of these curves is the strong asymmetry near the nadir when τ is small; in this region the radiance is always greater for $\phi = 180^{\circ}$ than the corresponding value for $\phi = 0^{\circ}$. Curves are not shown here for other values of ϕ, since the variation is relatively small.

The upward radiance when $\mu_0 = 0.1882$ and $A = 0$ is shown in Fig. 5 when $\phi = 0^{\circ}$ and 180°, in Fig. 6 when $\phi = 30^{\circ}$ and 150°, and in Fig. 3b when $\phi = 90^{\circ}$. There is the same asymmetry in the curves near the nadir when τ is small. The limiting curve for large τ shows a pronounced limb brightening at both horizons. The variation with ϕ is modest.

The upward radiance when $\mu_0 = 0.1882$ and $A = 0.2$ is given in Fig. 7 when $\phi = 0^{\circ}$ and 180° and in Fig. 8a when $\phi = 90^{\circ}$. The radiance when $\tau \ll 1$

is nearly independent of the nadir angle. On the other hand the limiting curve for large τ is nearly the same as when A = 0.

The upward radiance when $\mu_0 = 0.5379$ or $\mu_0 = 0.1882$ and A = 1 is shown in Fig. 9 when $\phi = 0^{\circ}$ and 180° and in Fig. 8b when $\phi = 90^{\circ}$. When $\tau \ll 1$ the upward radiance is nearly independent of μ, since almost all of the observed photons have been reflected from the Lambert surface. As τ increases more variation develops in the radiance curves for $\mu_0 = 0.1882$ than for $\mu_0 = 0.5379$. A slight limb brightening develops in the principal plane for $\mu_0 = 0.5379$ as τ increases, while a slight limb darkening arises at $\phi = 90^{\circ}$. For $\mu_0 = 0.1882$ there is a more pronounced limb brightening in the principal plane as τ increases together with an asymmetry in the curve around the nadir. The limb brightening is also present for $\phi = 90^{\circ}$.

The downward radiance when $\mu_0 = 1$ and A = 0, 0.2, and 1 is shown in Figs. 10a, 10b, and 11a respectively. As τ increases from a very small value, the downward radiance increases for a given μ value and reaches a maximum value when $\tau \sim 1$ for A = 0 and 0.2. Limb brightening also changes to limb darkening near $\tau = 1$. When A = 1 the downward radiance approaches a constant limiting value on the scale of these curves when $\tau \sim 16$; since there is no absorption either in the atmosphere or at the boundary surface, a uniform radiation field develops deep in such an atmosphere. A quantity of interest is the ratio of the downward radiance at the zenith to the value near the horizon (last computed point $\mu = 0.03785$ or $\theta = 87.83^{\circ}$) for large values of τ; this ratio is 2.713, 2.115, and 1.000 when A = 0, 0.2, and 1 respectively. The ratio is independent of the value of μ_0 in the limit of large τ.

The downward radiance in the principal plane when $\mu_0 = 0.5379$ is shown in Fig. 12. The same features appear in these curves as in those for $\mu_0 = 1$ already discussed. There is an asymmetry in the curves around the zenith direction when $\tau \leq 1$.

The downward radiance when $\mu_0 = 0.1882$ and $A = 0$ is shown in Fig. 13 when $\phi = 0^o$ and 180^o and in Fig. 11b when $\phi = 90^o$. Because of the low solar angle, the maximum value of the downward radiance for μ values near the horizon now occurs for values of the optical thickness appreciably less than unity.

The downward radiance when $\mu_0 = 0.1882$ and $A = 0.2$ is shown in Fig. 14 for the principal plane and in Fig. 15a for $\phi = 90^o$. These curves are very similar to the corresponding curves for $A = 0$. The downward radiance is not sensitive to the value of the surface albedo in this range, since a photon reflected from the surface into an upward direction must be scattered another time in order to join the downward stream of radiation.

The downward radiance when $\mu_0 = 0.5379$ and $A = 1$ is given in Fig. 16 for the principal plane. The curves for $\tau \ll 1$ have the same shape as those for $A = 0$ and 0.2, but the actual radiance values are greater. The downward radiance for $A = 1$ is essentially independent of μ when τ is much larger than unity.

The downward radiance for $\mu_0 = 0.1882$ and $A = 1$ is shown in Fig. 17 for $\phi = 0^o$ and 180^o and in Fig. 15b for $\phi = 90^o$. The main difference between these curves and those for solar angles nearer the zenith is that the downward radiance near the horizon for $\mu_0 = 0.1882$ is appreciably greater than its limiting value for large τ over a range of τ values from approximately 0.02 to 1. For τ values larger than unity the radiance approaches a constant limiting value independent of μ.

4. Conclusion

A modified version of the discrete ordinate theory of radiative transfer has been presented here. This theory has relatively simple expressions for the radiance at any depth in a plane parallel atmosphere with each term representing a physical interaction appropriate to the problem. No iteration procedures are used, but rather all orders of multiple scattering are calculated at once. This theory can be used when the atmospheric parameters vary with height, since layers of any desired thicknesses may be combined. The radiance may readily be calculated for large optical depths, highly anisotropic phase functions, for all values of the surface albedo including $A = 1$ and for a number of polar angles including $\mu = 1$. As a first application of the method detailed results have been given for Rayleigh scattering from a homogeneous layer. The upward and downward radiance is given for optical thicknesses τ from 0.0019 to 4096, for surface albedo $A = 0$, 0.2, and 1, and for cosine of solar zenith angle $\mu = 1$, 0.5379, and 0.1882. This work was supported in part by Grant No. NGR 44-001-117 from the National Aeronautics and Space Administration.

REFERENCES

1. Chandrasekhar,S. 1960: Radiative Transfer. New York, Dover Publications, Inc., 393 pp.

2. Coulson, K. L., J. V. Dave, and Z. Sekera, 1960; Tables Related to Radiation Emerging from a Planetary Atmosphere with Rayleigh Scattering. Berkeley and Los Angeles, University of California Press, 548 pp.

3. Dave, J. V., 1970: Intensity and polarization of the radiation emerging from a plane-parallel atmosphere containing monodispersed aerosols. Appl. Opt. 9, 2673-2684.

4. Dave, J. V. and P. M. Furukawa, 1966: Intensity and polarization of the radiation emerging from an optically thick Rayleigh atmosphere. 56, 394-400.

5. Dave, J. V. and J. Gazdag, 1970: A modified Fourier transform method for multiple scattering calculations in a plane parallel Mie atmosphere. Appl. Opt. 9, 1457-1466.

6. Fymat, A. L. and K. D. Abhyankar, 1971: Effect of absorption on scattering by planetary atmospheres. J. Geophys. Res. 76, 732-735.

7. Grant, I. P. and G. E. Hunt: 1969: Discrete space theory of radiative transfer. Proc. Roy. Soc. Lond. A313, 183-216.

8. Hansen, J. E., 1969a: Radiative transfer by doubling in very thin layers. Astrophy. J. 155, 565-573.

9. Hansen, J. E., 1969b: Exact and approximate solutions for multiple scattering by cloudy and hazy planetary atmospheres. J. Atmos. Sci. 26, 478-487.

10. Hansen, J. E., 1971a: Multiple scattering of polarized light in planetary atmospheres. Part I. The doubling method. J. Atmos Sci. 28, 120-125.

11. Hansen, J. E., 1971b: Multiple scattering of polarized light in planetary atmospheres. Part II. Sunlight reflected by terrestrial water clouds. J. Atmos. Sci. 28 (scheduled for Nov., 1971 issue).

12. Hansen, J. E. and J. B. Pollack, 1970: Near-infrared light scattering by terrestrial clouds. J. Atmos. Sci., 27, 265-281.

13. Herman, B. M. and S. R. Browning, 1965: A numerical solution to the equation of radiative transfer. J. Atmos. Sci., 22, 559-566.

14. Herman, B. M., S. R. Browning, and R. J. Curran, 1971: The effect of atmospheric aerosols on scattered sunlight. J. Atmos. Sci., 28, 419- 428.

15. Howell, H. B. and H. Jacobowitz, 1970: Matrix method applied to the multiple scattering of polarized light. J. Atmos. Sci., 27, 1195-1206.

16. Kahle, A. B., 1968a: Intensity of radiation from a Rayleigh-scattering atmosphere. J. Geophy. Res., 73, 7511-7518.

17. Kahle, A. B., 1968b: Global radiation emerging from a Rayleigh-scattering atmosphere of large optical thickness. Astrophy. J., 151, 637-645.

18. Kourganoff, V., 1952: Basic Methods in Transfer Problems. Oxford, England, Clarendon Press, 281 pp.

19. Preisendorfer, R. W., 1965: Radiative Transfer on Discrete Spaces. New York, Pergamon Press, 459 pp.

20. Sekera, Z., 1956: Recent developments in the study of the polarization of skylight. Advan. Geophy. 3, 43-104.

21. Sekera, Z., 1957: Polarization of skylight, in Handbuch der Physik, edited by S. Fluuge. Berlin, Springer-Verlag, Vol. 48, p. 288-328.

22. Stroud, A. H., and D. Secrest., 1966: Gaussian Quadrature Formulas. New Jersey, Prentice Hall, 374 pp.

23. Twomey, S., H. Jacobowitz, and H. B. Howell, 1966: Matrix methods for multiple-scattering problems. J. Atmos. Sci., 23, 289-296.

24. Twomey, S., H. Jacobowitz, and H. B. Howell, 1967: Light scattering by cloud layers. J. Atmos. Sci., 24, 70-79.

Legends for Figures

Fig. 1. Graphic representation of discrete ordinate vectors.

Fig 2. Upward radiance at the top of atmosphere for Rayleigh scattering for $\mu_o = 1$ and various values of the optical thickness τ as a function of the cosine of the nadir angle μ. The left hand figure is for $A = 0$ (Fig. 2a); the right hand figure is for $A = 0.2$ (Fig. 2b). The limiting curve for large τ is the same as the last plotted curve within the width of the symbols.

Fig. 3a. Upward radiance for $\mu_o = 1$ and $A = 1$; Fig. 3b. $\mu_o = 0.1882$, $A = 0$, and $\phi = 90°$. See Fig. 2 for key.

Fig. 4. Upward radiance for $\mu_o = 0.5379$, $A = 0$, and $\phi = 0°$ and $180°$. See Fig. 2 for key.

Fig. 5. Upward radiance for $\mu_o = 0.1882$, $A = 0$, and $\phi = 0°$ and $180°$. See Fig. 2 for key.

Fig. 6. Upward radiance for $\mu_o = 0.1882$, $A = 0$, and $\phi = 30°$ and $150°$. See Fig. 2 for key.

Fig. 7. Upward radiance for $\mu_o = 0.1882$, $A = 0.2$, and $\phi = 0°$ and $180°$. See Fig. 2 for key.

Fig. 8a. Upward radiance for $\mu_o = 0.1882$, $A = 0.2$, and $\phi = 90°$; Fig. 8b. $\mu_o = 0.5379$ and 0.1882, $A = 1$, and $\phi = 90°$. See Fig. 2 for key.

Fig. 9. Upward radiance for $\mu_o = 0.5379$ and 0.1882, $A = 1$, and $0°$ and $180°$. See Fig. 2 for key.

Fig. 10a. Downward radiance at bottom of atmosphere for $\mu_o = 1$ and $A = 0$; Fig. 10b. $\mu_o = 1$ and $A = 0.2$. See Fig. 2 for key.

Fig. 11a. Downward radiance for $\mu_o = 1$ and $A = 1$; Fig. 11b. $\mu_o = 0.1882$, $A = 0$, and $\phi = 90°$. See Fig. 2 for key.

Fig. 12. Downward radiance for $\mu_o = 0.5379$, $A = 0$, and $\phi = 0°$ and $180°$. See Fig. 2 for key.

Fig. 13. Downward radiance for $\mu_o = 0.1882$, $A = 0$, and $\phi = 0°$ and $180°$. See Fig. 2 for key.

Fig. 14. Downward radiance for $\mu_o = 0.1882$, $A = 0.2$, and $\phi = 0°$ and $180°$. See Fig. 2 for key.

Fig. 15a. Downward radiance for $\mu_o = 0.1882$, $A = 0.2$, and $\phi = 90°$; Fig. 15b. $\mu_o = 0.1882$, $A = 1$, and $\phi = 90°$. See Fig. 2 for key.

Fig. 16. Downward radiance for $\mu_o = 0.5379$, $A = 1$, and $\phi = 0°$ and $180°$. See Fig. 2 for key.

Fig. 17. Downward radiance for $\mu_o = 0.1882$, $A = 1$, and $\phi = 0°$ and $180°$. See Fig. 2 for key.

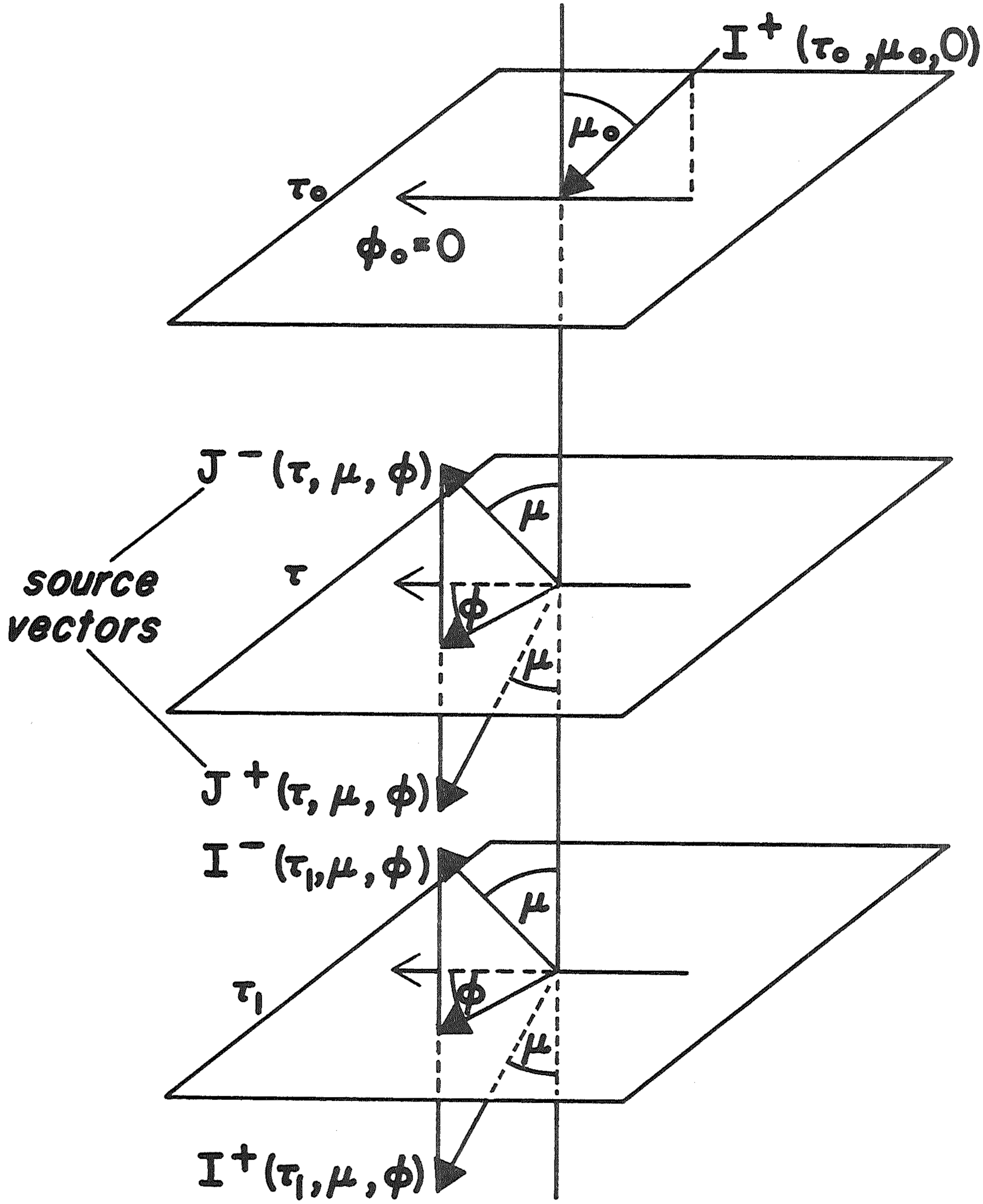

$I^+(\tau_0, \mu_0, 0)$
μ_0
τ_0
$\phi_0 = 0$
$J^-(\tau, \mu, \phi)$
μ
source vectors
τ
ϕ
μ
$J^+(\tau, \mu, \phi)$
$I^-(\tau_1, \mu, \phi)$
μ
τ_1
ϕ
μ
$I^+(\tau_1, \mu, \phi)$

Figure 1

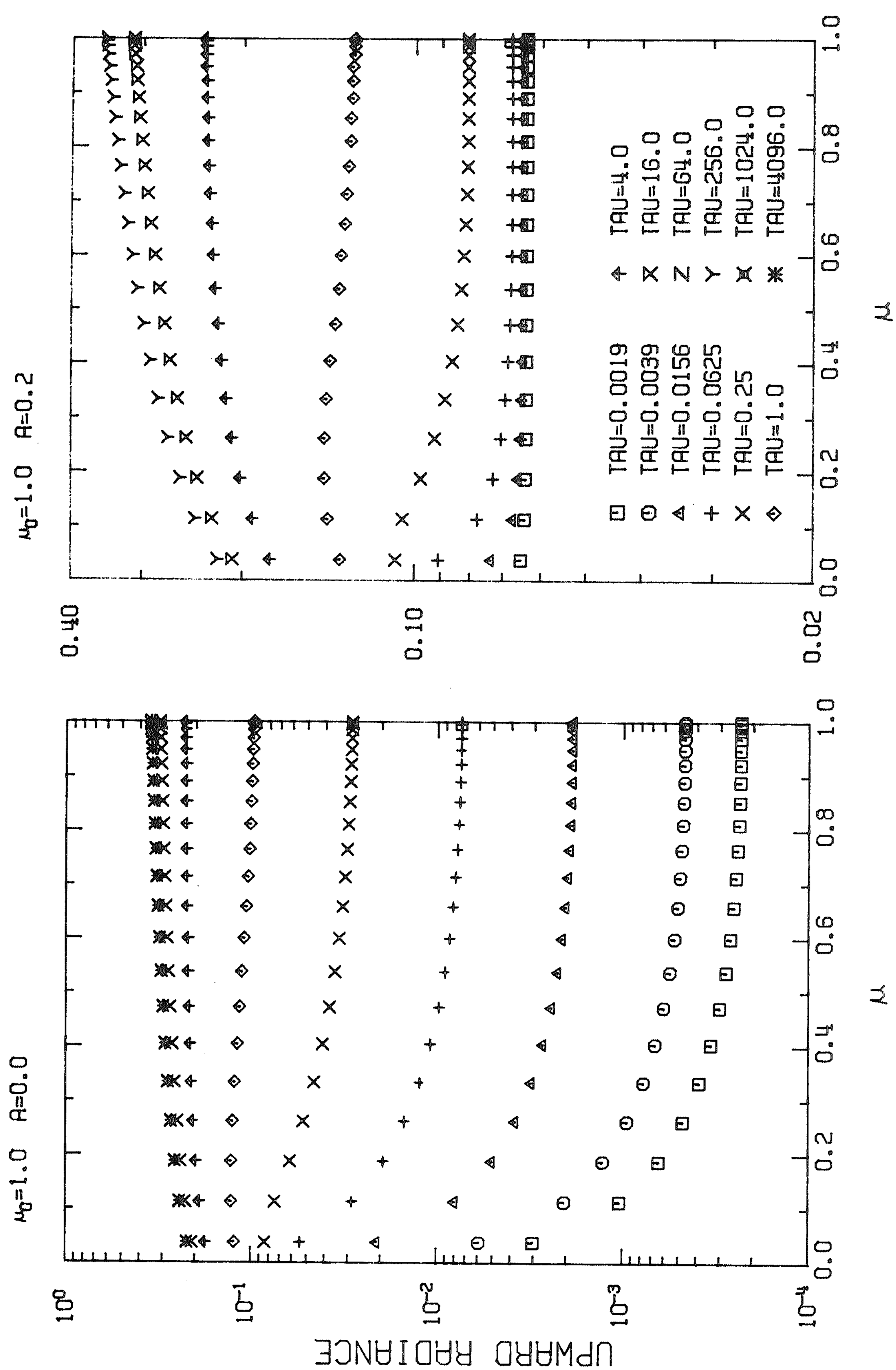

Figure 2a and 2b

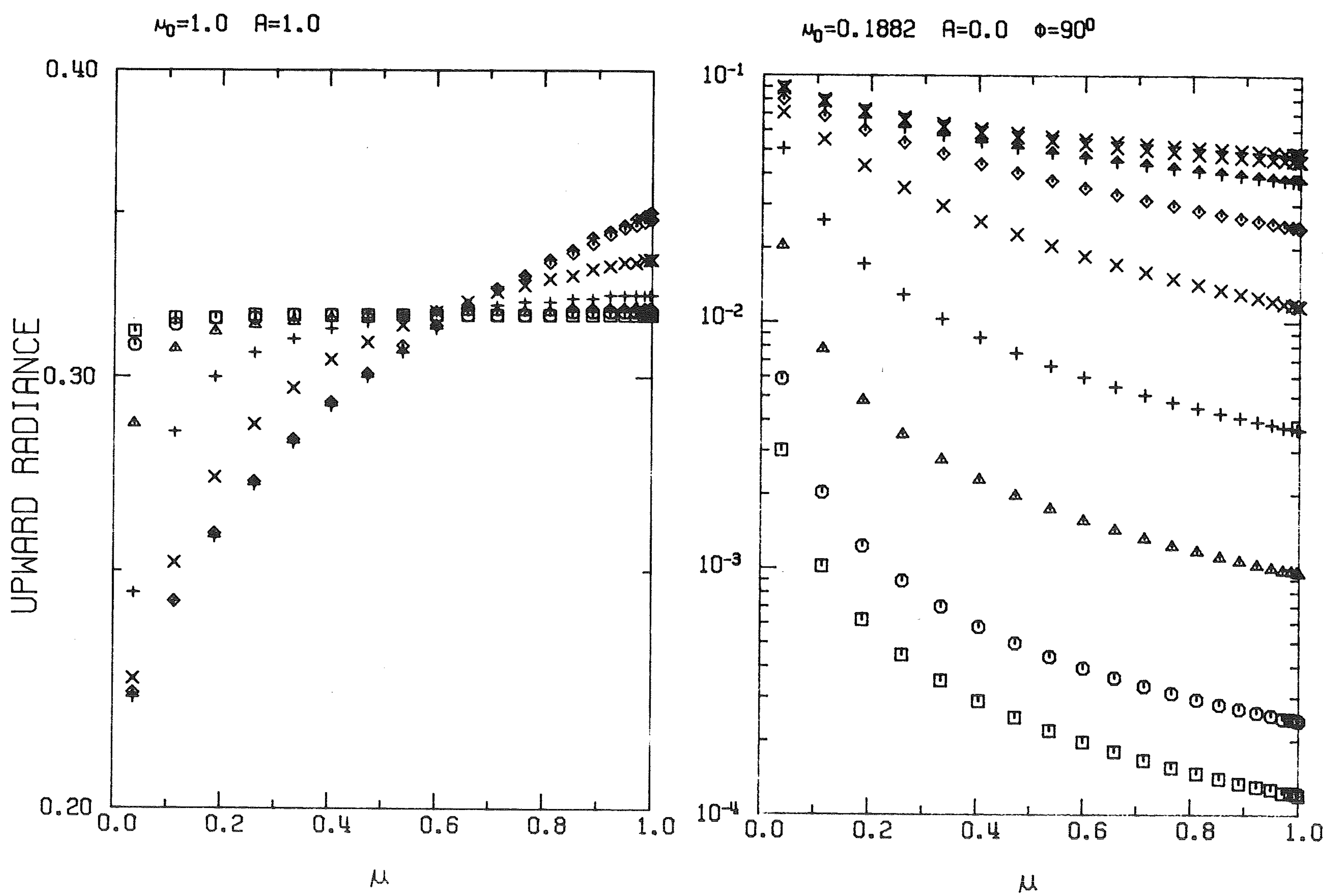

Figure 3a and 3b

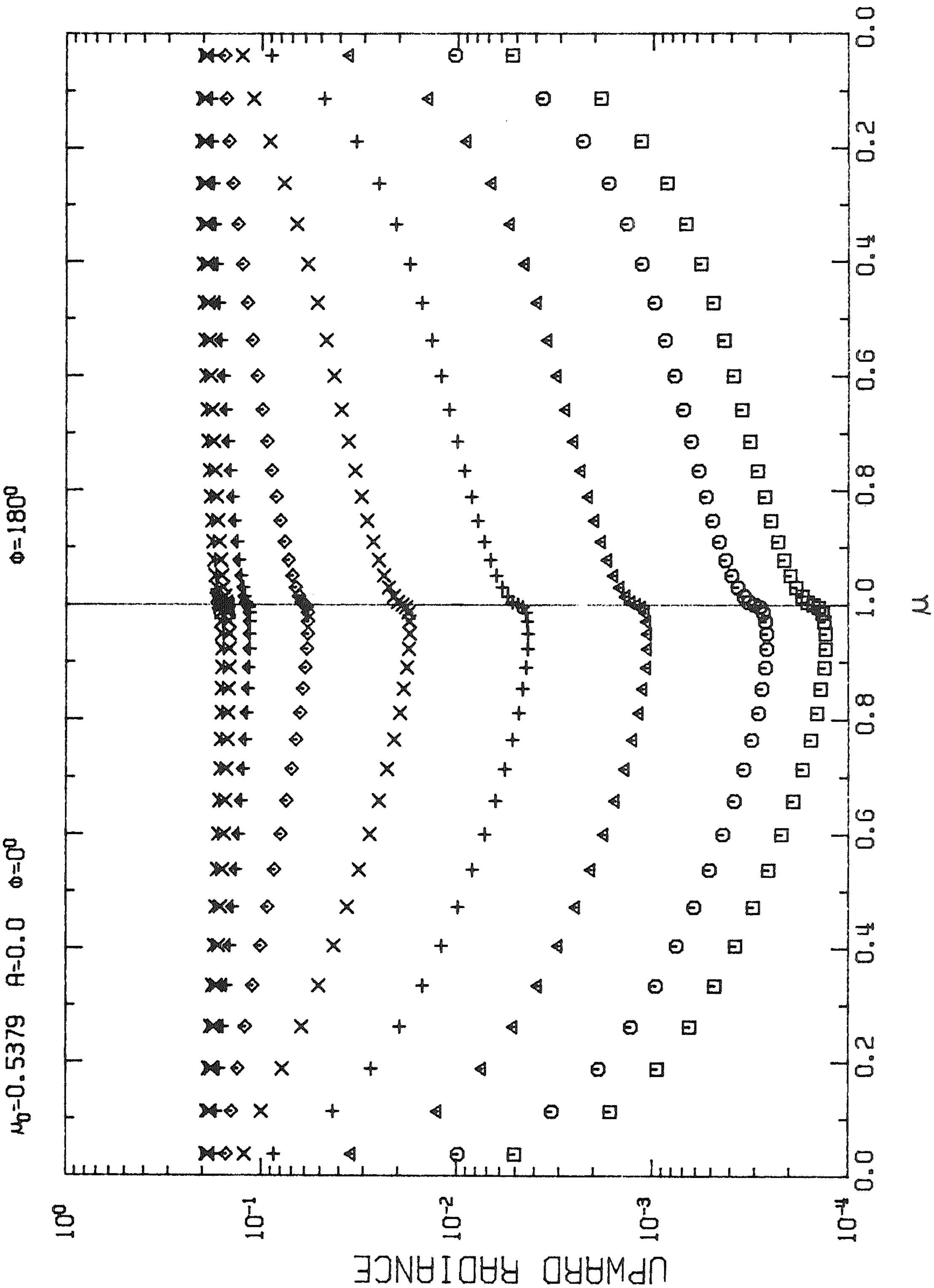

Figure 4

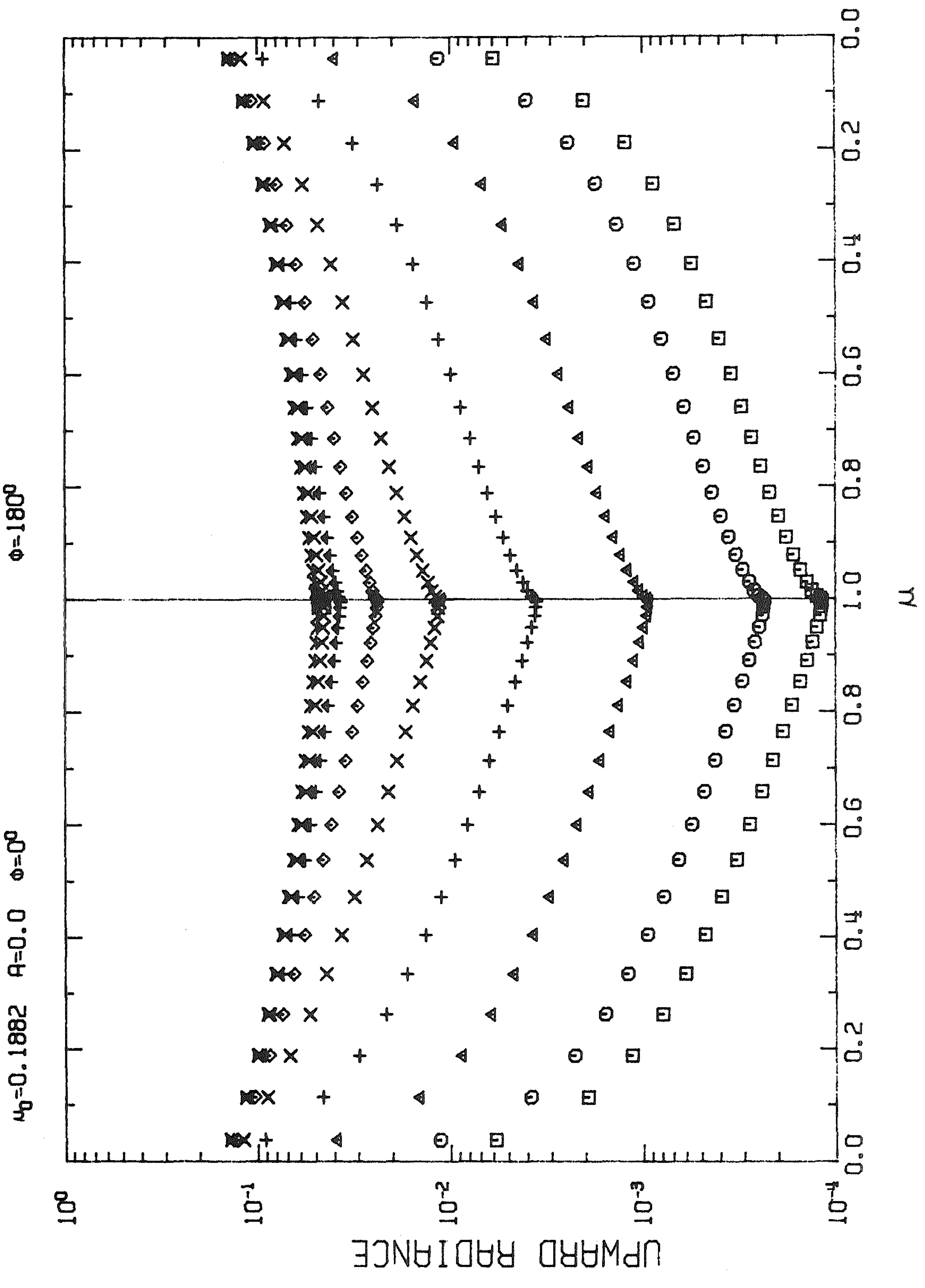
μ0=0.1882 A=0.0 Φ=0°
Φ=180°
UPWARD RADIANCE
μ
10^0
10^-1
10^-2
10^-3
10^-4
0.0
0.2
0.4
0.6
0.8
1.0
0.8
0.6
0.4
0.2
0.0

Figure 5

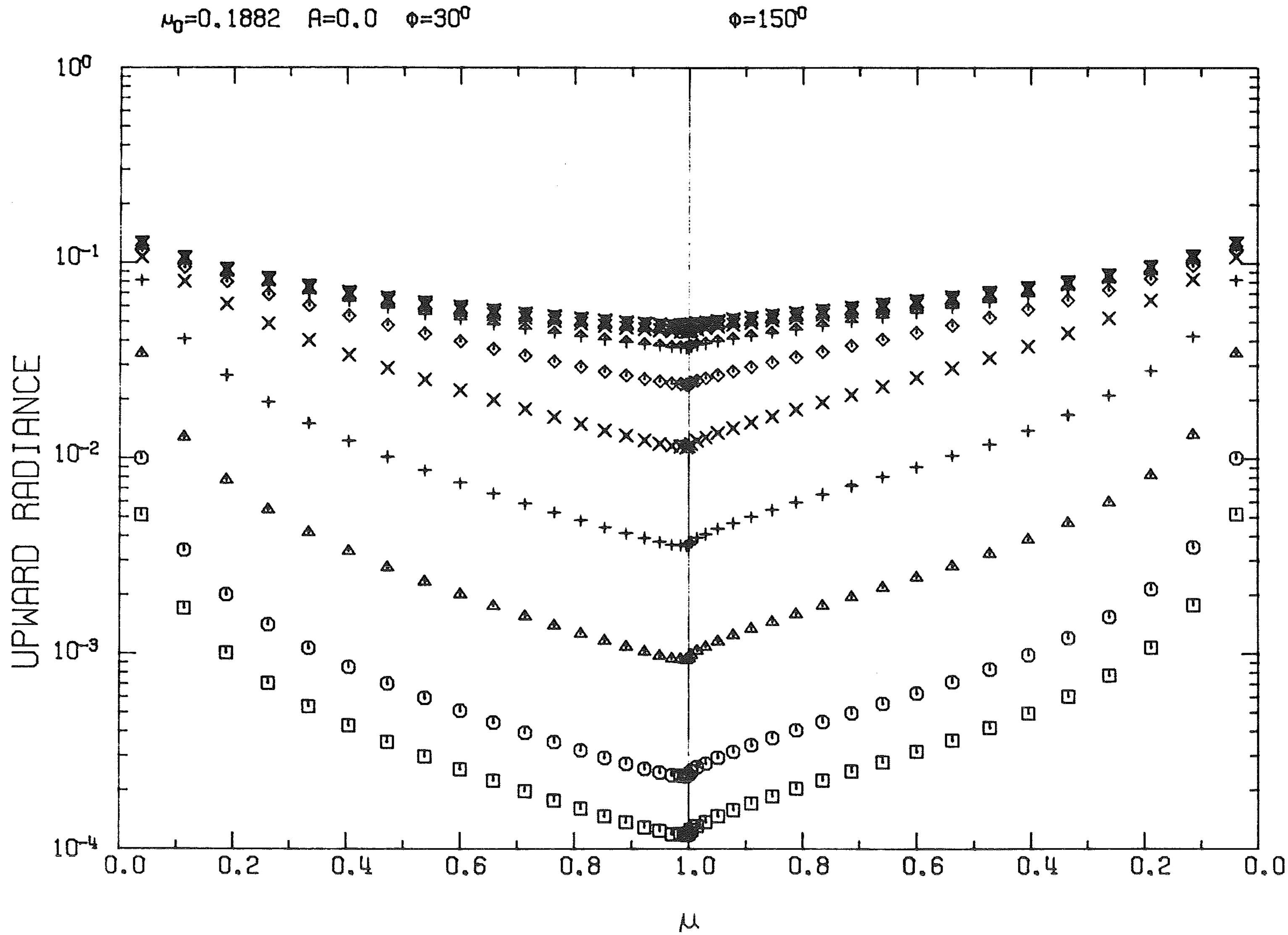
μ_0=0.1882 A=0.0 Φ=30^0
Φ=150^0
UPWARD RADIANCE
10^0
10^{-1}
10^{-2}
10^{-3}
10^{-4}
0.0
0.2
0.4
0.6
0.8
1.0
0.8
0.6
0.4
0.2
0.0
μ

Figure 6

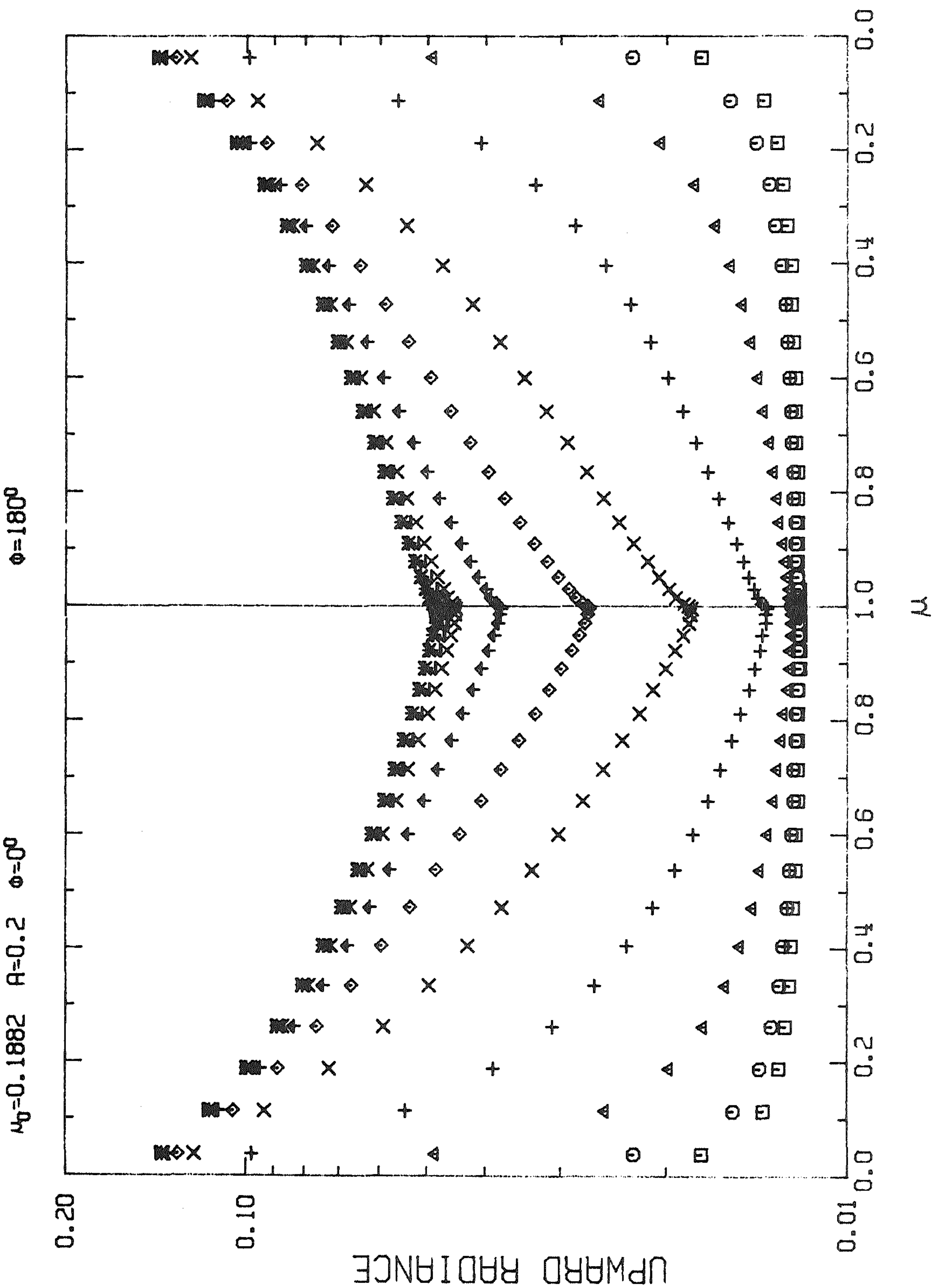

μ0=0.1882 A=0.2 Φ=0°
Φ=180°
UPWARD RADIANCE
0.20
0.10
0.01
0.0
0.2
0.4
0.6
0.8
1.0
0.8
0.6
0.4
0.2
0.0
μ

Figure 7

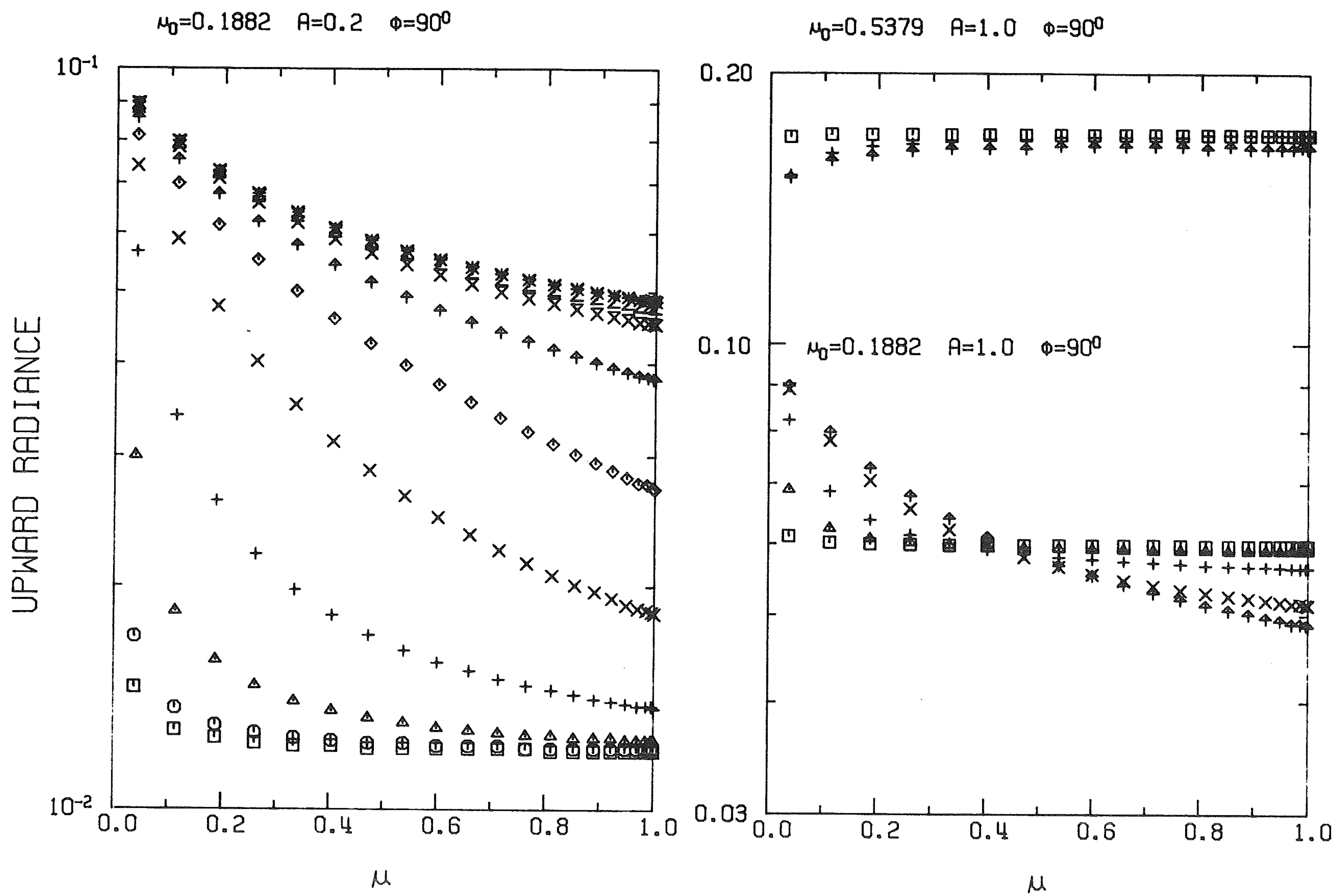

Figure 8a and 8b

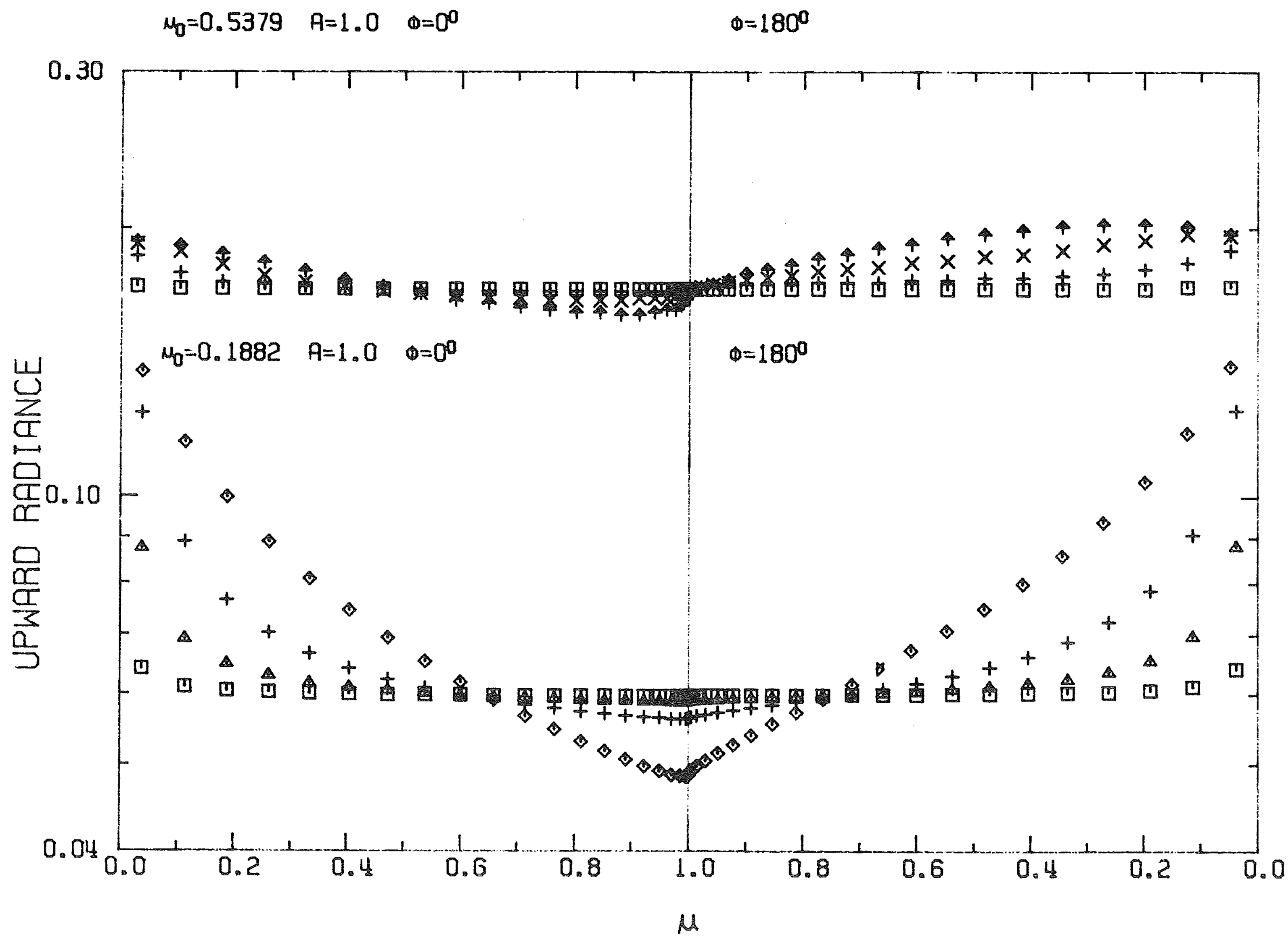
μ0=0.5379 A=1.0 Φ=0°
Φ=180°
μ0=0.1882 A=1.0 Φ=0°
Φ=180°
UPWARD RADIANCE
0.30
0.10
0.04
0.0
0.2
0.4
0.6
0.8
1.0
0.8
0.6
0.4
0.2
0.0
μ

Figure 9

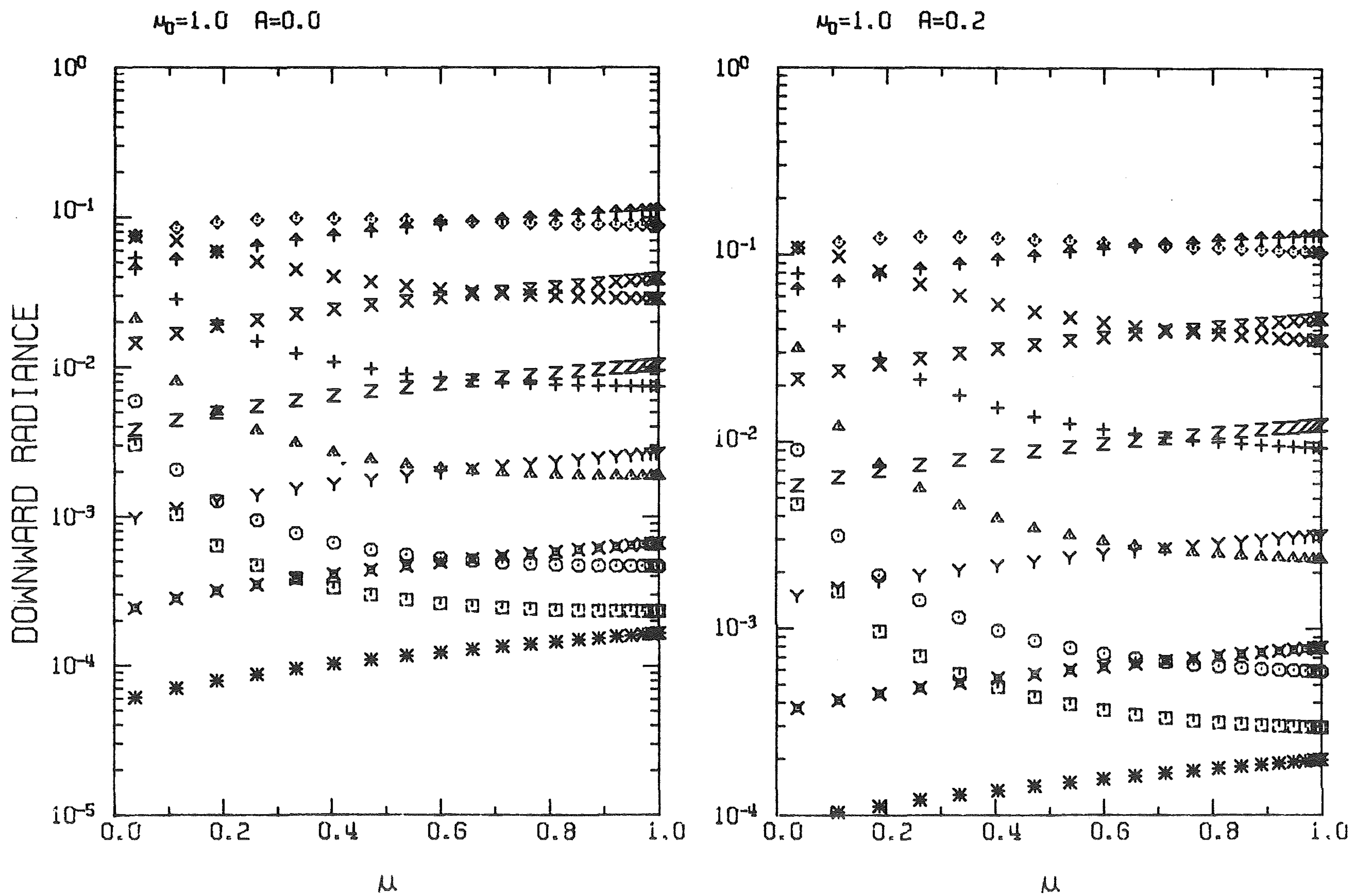

Figure 10a and 10b

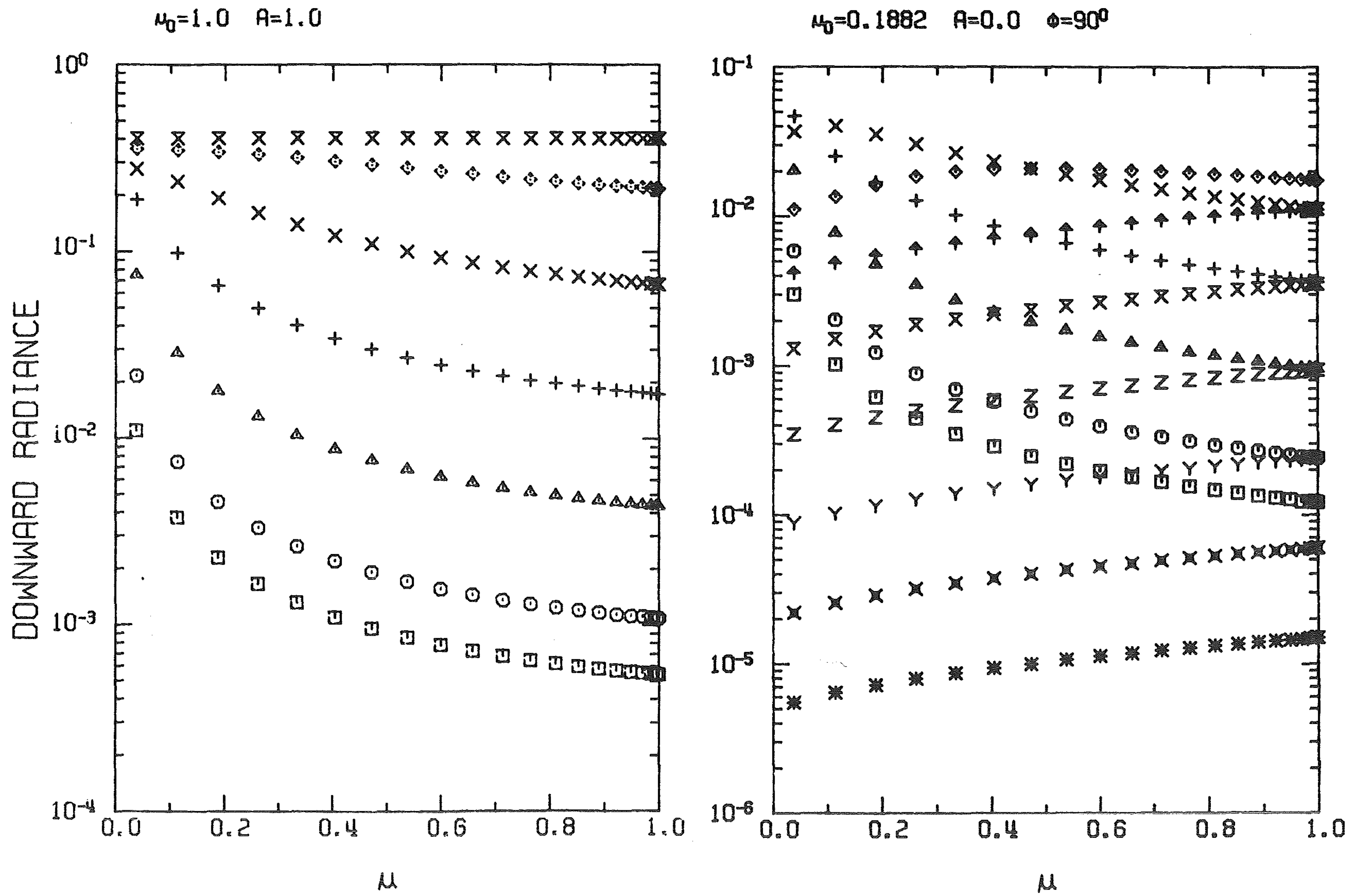

Figure 11a and 11b

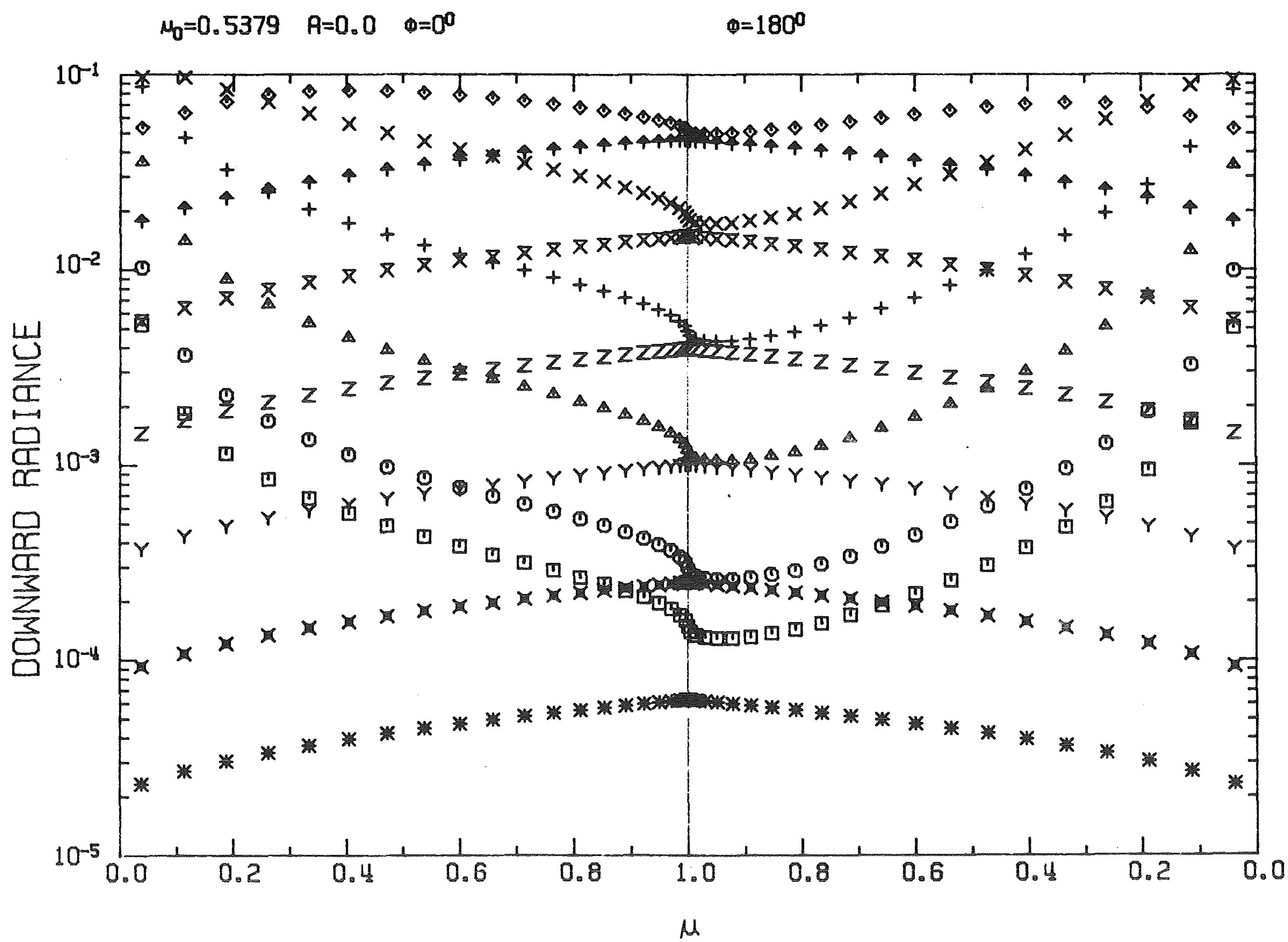

μ0=0.5379 A=0.0 Φ=0°
Φ=180°
DOWNWARD RADIANCE
10^-1
10^-2
10^-3
10^-4
10^-5
0.0 0.2 0.4 0.6 0.8 1.0 0.8 0.6 0.4 0.2 0.0
μ

Figure 12

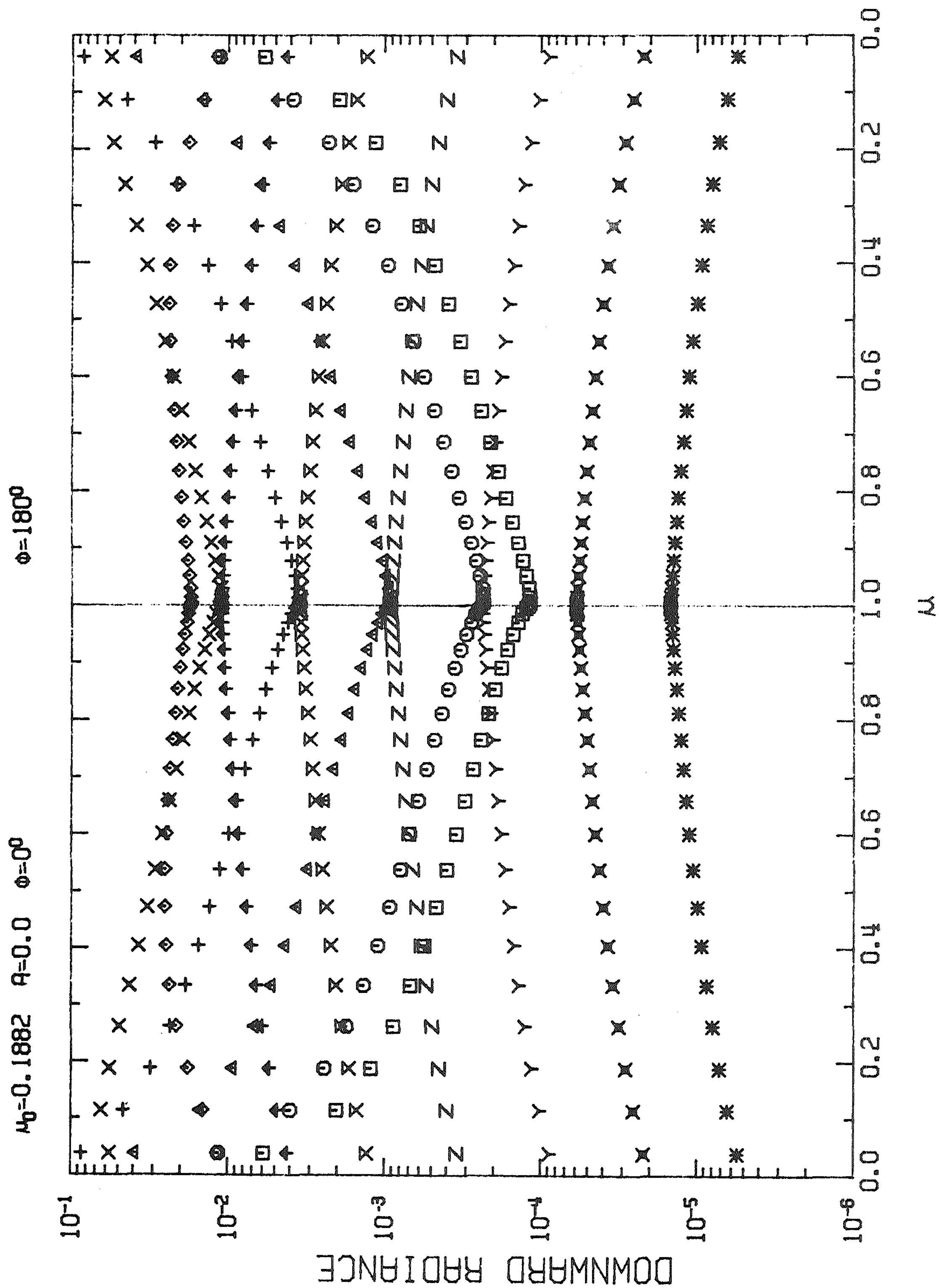

μ0=0.1882 A=0.0 Φ=0°
Φ=180°
DOWNWARD RADIANCE
10^-1
10^-2
10^-3
10^-4
10^-5
10^-6
0.0
0.2
0.4
0.6
0.8
1.0
0.8
0.6
0.4
0.2
0.0
μ

Figure 13

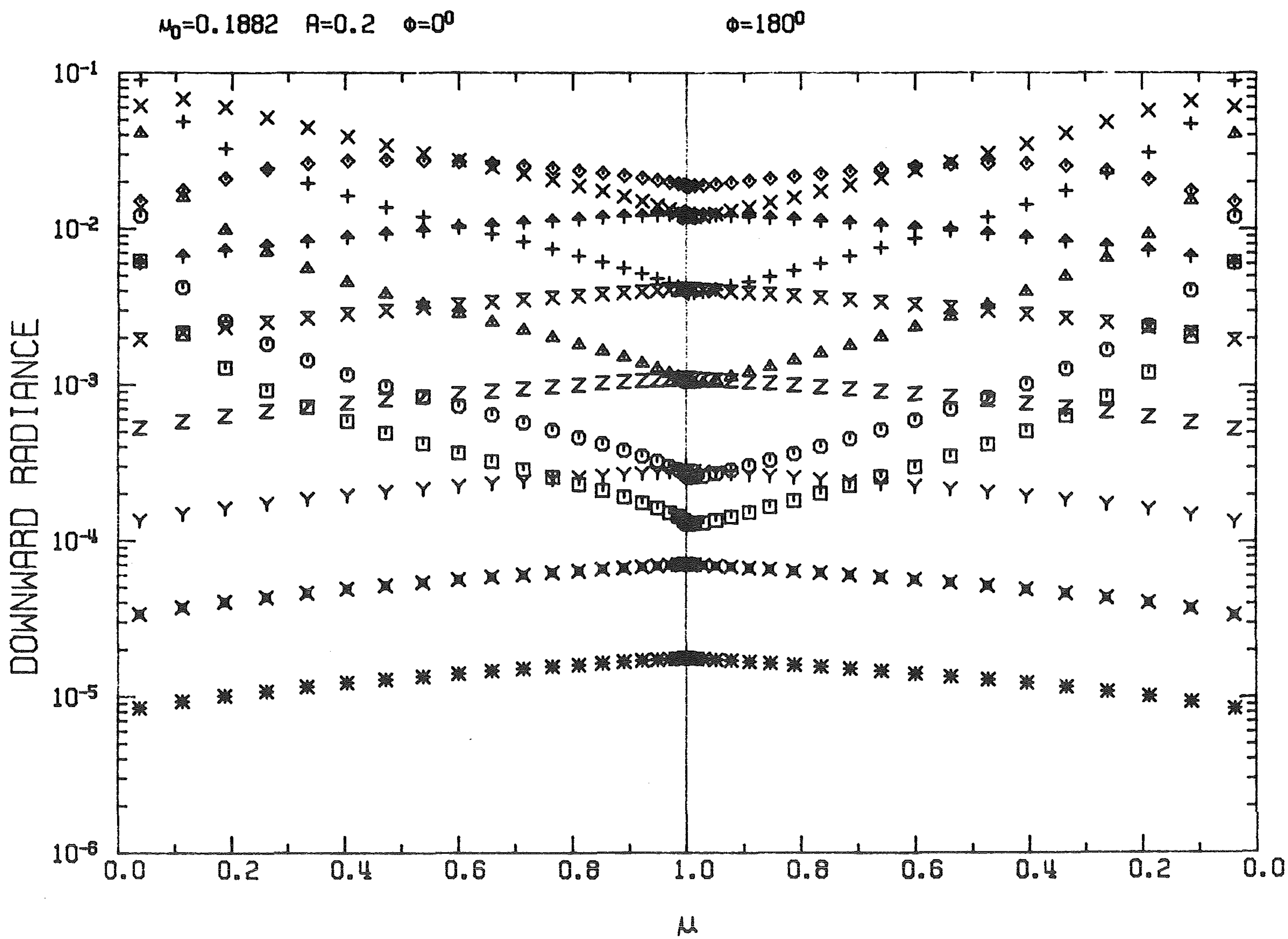

μ_0=0.1882 A=0.2 Φ=0°
Φ=180°
DOWNWARD RADIANCE
10^-1
10^-2
10^-3
10^-4
10^-5
10^-6
0.0
0.2
0.4
0.6
0.8
1.0
0.8
0.6
0.4
0.2
0.0
μ

Figure 14

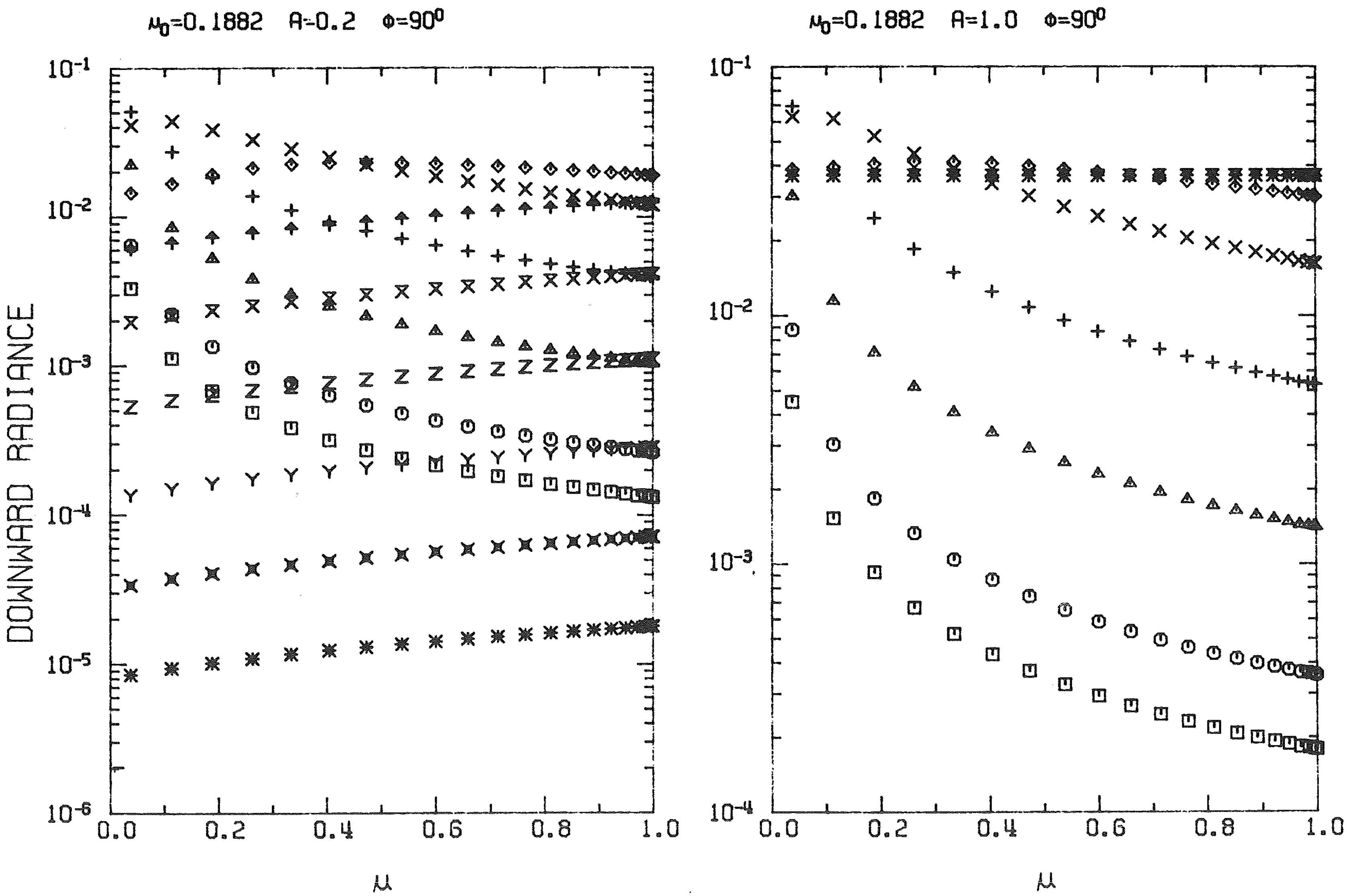

Figure 15a and 15b

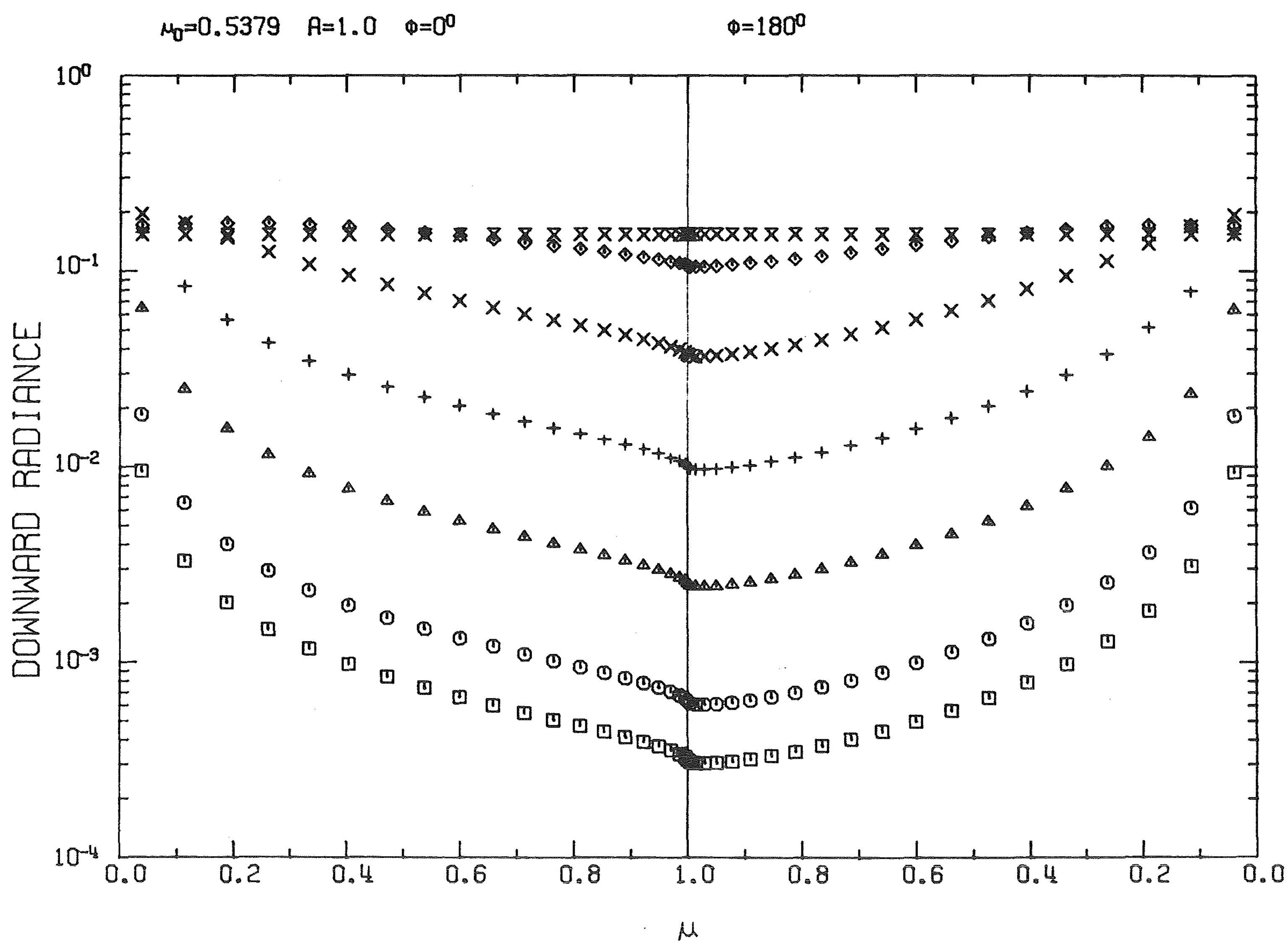

μ_0=0.5379 A=1.0 Φ=0°
Φ=180°
DOWNWARD RADIANCE
10^0
10^{-1}
10^{-2}
10^{-3}
10^{-4}
0.0 0.2 0.4 0.6 0.8 1.0 0.8 0.6 0.4 0.2 0.0
μ

Figure 16

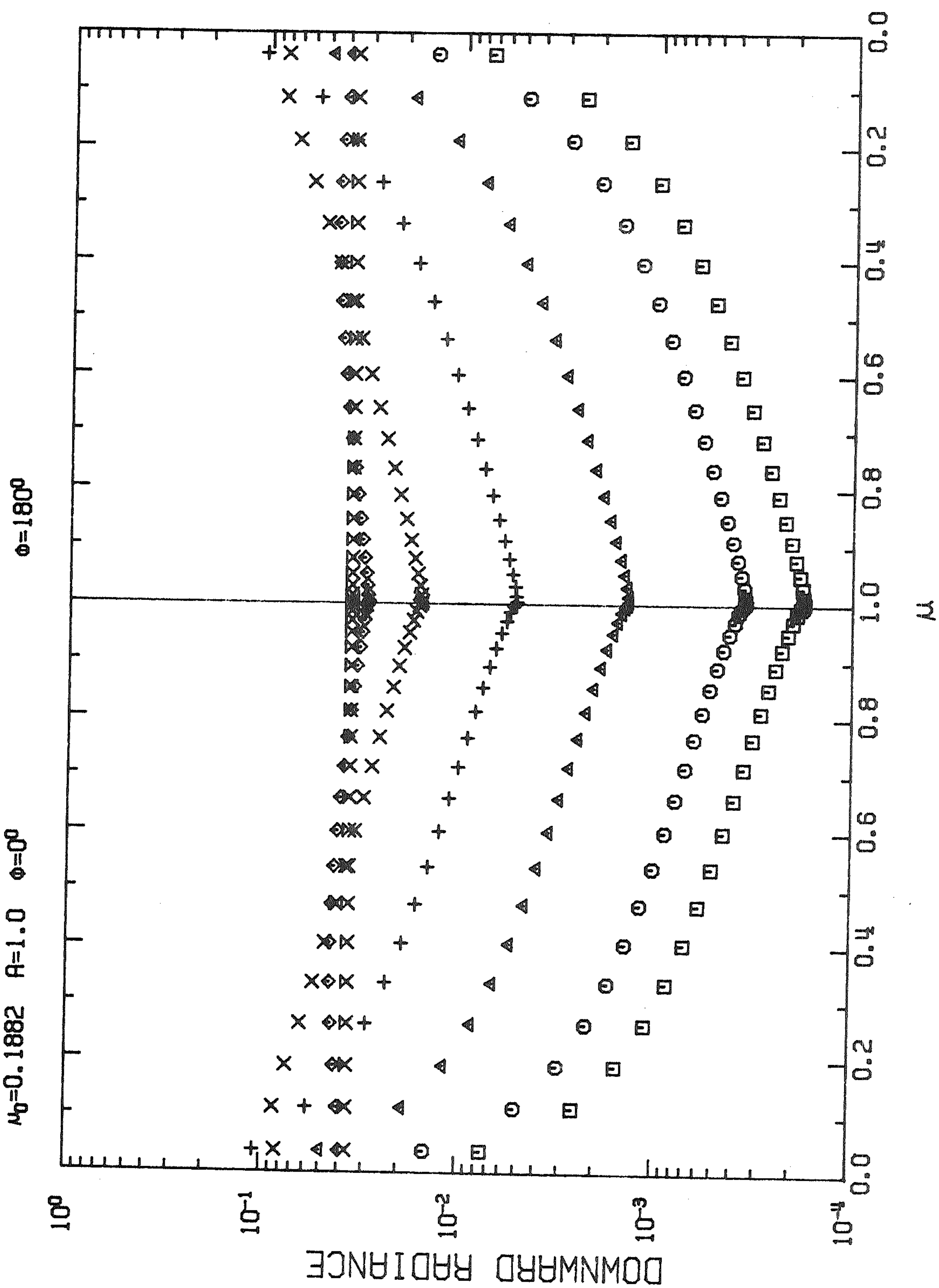

μ_0=0.1882 A=1.0 Φ=0°
Φ=180°
DOWNWARD RADIANCE
μ
10^0
10^{-1}
10^{-2}
10^{-3}
10^{-4}
0.0
0.2
0.4
0.6
0.8
1.0
0.8
0.6
0.4
0.2
0.0

Figure 17